

Amphiphilic Distyrylbenzene Derivatives as Potential Therapeutic and Imaging Agents for the Soluble Amyloid- β Oligomers in Alzheimer's Disease

Liang Sun,¹ Hong-Jun Cho,¹ Soumyo Sen,³ Andres S. Arango,³ Truc T. Huynh,^{4,5} Yiran Huang,¹ Nilantha Bandara,⁴ Buck E. Rogers,⁴ Emad Tajkhorshid,³ and Liviu M. Mirica^{1,2,*}

¹ Department of Chemistry, Beckman Institute for Advanced Science and Technology, The Neuroscience Program, University of Illinois at Urbana-Champaign, 600 S. Mathews Avenue, Urbana, Illinois 61801, United States

² Hope Center for Neurological Disorders, Washington University School of Medicine, St. Louis, MO 63110, United States

³ NIH Center for Macromolecular Modeling and Bioinformatics, Beckman Institute for Advanced Science and Technology, Center for Biophysics and Quantitative Biology and Department of Biochemistry, University of Illinois at Urbana-Champaign, Urbana, IL 61801, United States

⁴ Department of Radiation Oncology, Washington University School of Medicine, St. Louis, Missouri 63108, United States

⁵ Department of Chemistry, Washington University, St. Louis, Missouri 63130, United States

*e-mail: mirica@illinois.edu.

Abstract

Alzheimer's Diseases (AD) is the most common neurodegenerative disease, but efficient therapeutic and early diagnosis agents for this neurological disorder are still lacking. Herein, we report the development of a novel amphiphilic compound, LS-4, generated linking a hydrophobic amyloid fibril-binding fragment with a hydrophilic azamacrocycle that can dramatically increase the binding affinity towards various amyloid β ($A\beta$) peptide aggregates. The developed compound exhibits uncommon fluorescence turn-on and high binding affinity for $A\beta$ aggregates, especially for soluble $A\beta$ oligomers. Moreover, upon the administration of LS-4 to 5xFAD mice, fluorescence imaging of the LS-4-treated brain sections reveals that LS-4 can readily penetrate the blood-brain-barrier (BBB) and bind to the $A\beta$ oligomers *in vivo*, as confirmed by immunostaining with an $A\beta$ oligomer-specific antibody. In addition, the treatment of 5xFAD mice with LS-4 significantly reduces the amount of both amyloid plaques and associated phosphorylated tau (p-tau) aggregates vs. the vehicle-treated 5xFAD mice, while microglia activation is also reduced. Furthermore, molecular dynamics simulations corroborate the observation that introducing a hydrophilic moiety into the molecular structure can significantly enhance the electrostatic interactions with the polar residues of the $A\beta$ peptide species. Finally, taking advantage of the strong Cu-chelating property of the azamacrocycle, we performed a series of radioimaging and biodistribution studies that show the ^{64}Cu -LS-4 complex binds to the amyloid plaques and can accumulate a significantly larger extent in the 5xFAD mice brains vs. the WT controls. Overall, these *in vitro* and *in vivo* studies illustrate that the novel strategy to employ an amphiphilic molecule containing a hydrophilic fragment attached to a hydrophobic amyloid fibril-binding fragment can increase the binding affinity of these compounds for the soluble $A\beta$ oligomers and can thus be used to detect and regulate the soluble $A\beta$ species in AD.

Keywords

Alzheimer's Disease; soluble amyloid- β ($A\beta$) oligomers; fluorescence imaging; amphiphilic molecules; microglia activation; phosphorylated tau aggregation; positron emission tomography (PET).

Introduction

Alzheimer's Disease (AD), the most prevalent neurodegenerative disease, currently affects almost 6 million people in the US and 44 million worldwide.¹ Unfortunately, AD is still an irremediable disorder with a complex pathology, which poses tremendous challenges for the development of therapeutic and diagnostic tools for AD.^{2,3} The formation of extracellular amyloid plaques containing the amyloid β (A β) peptide is one of the pathological hallmarks of the brains of AD patients,^{4,5} and this led to the amyloid-cascade hypothesis that states the amyloid plaque formation initiates cellular events that lead to neurodegeneration.⁶⁻⁷ However, recent studies indicate that the deposition of amyloid plaques does not correlate with the progression of AD, instead, soluble A β oligomers are believed to play a significant role in the cause of the disease, as they lead to synaptic dysfunction and memory loss in AD patients and AD animal models.^{8,9}

Fluorescence probes for amyloid fibrils have been developed and widely used during the past two decades.¹⁰⁻¹³ These probes can specifically bind to the amyloid plaques in AD patients and AD models. Furthermore, several positron emission tomography (PET) compounds have been developed and approved by the FDA and can be used to visualize amyloid plaques in AD patients.¹⁴⁻¹⁶ The main strategy to develop such imaging agents is to employ hydrophobic π -conjugated aromatic systems that interact with the hydrophobic residues in the β -sheet cores of the amyloid fibrils through hydrophobic-hydrophobic interactions. However, most of the probes can only recognize the insoluble A β species and have a poor ability to detect soluble A β oligomers, thus limiting their applicability for early AD diagnosis.

Recently, novel fluorescent dyes that can selectively bind soluble A β oligomers have been reported.¹⁷⁻²⁴ However, the discovery of these molecules is normally achieved via high throughput

screening (HTS) or limited structure-activity relationship (SAR) studies, and there are no general guidelines to rationally design a soluble A β oligomer probe. In addition, numerous studies have shown that multifunctional compounds (MFCs) that contain an A β fibril-binding fragment and additional moieties that target other AD pathologies such as metal ion dishomeostasis,²⁵⁻³⁰ reactive oxygen species (ROS) species formation,³¹⁻³³ neuroinflammation,³⁴⁻³⁵ acetylcholinesterase inhibition,³⁶⁻³⁷ have proven to be a highly efficient therapeutic strategy for AD.³⁸⁻⁴² However, to the best of our knowledge to date no MFCs have been developed that should exhibit selectivity for the soluble A β oligomers and target also other AD pathologies.

Herein, we report the development of a novel amphiphilic compound, LS-4, generated by linking a hydrophobic amyloid fibril-binding fragment with a hydrophilic azamacrocycle that can dramatically increase the binding affinity towards various amyloid β (A β) peptide aggregates (Figure 1). The developed compound exhibits uncommon fluorescence turn-on and high binding affinity for A β aggregates, especially for soluble A β oligomers. By comparison, the compound Pre-LS-4, which contains only the hydrophobic conjugated aromatic fragment without the hydrophilic azamacrocycle moiety, exhibits significantly reduced binding affinity for the A β species. Moreover, upon the administration of LS-4 to 5xFAD mice, fluorescence imaging of the LS-4-treated brain sections reveals that LS-4 can readily penetrate the blood-brain-barrier (BBB) and bind to the A β oligomers *in vivo*, as confirmed by immunostaining with an A β oligomer-specific antibody. In addition, the treatment of 5xFAD mice with LS-4 significantly reduces the amount of both amyloid plaques and associated phosphorylated tau (p-tau) aggregates vs. the vehicle-treated 5xFAD mice, while microglia activation is also reduced. Furthermore, molecular dynamics (MD) simulations corroborate the observation that introducing a hydrophilic moiety into the molecular structure can significantly enhance the electrostatic interactions with the polar

residues of the A β peptide species. Finally, taking advantage of the strong Cu-chelating property of the azamacrocycle, we performed a series of radioimaging and biodistribution studies that show the ^{64}Cu -LS-4 complex binds to the amyloid plaques and can accumulate a significantly larger extent in the 5xFAD mice brains vs. the WT controls. Overall, these *in vitro* and *in vivo* studies illustrate that the novel strategy to employ an amphiphilic molecule containing a hydrophilic fragment attached to a hydrophobic amyloid fibril-binding fragment can increase the binding affinity of these compounds for the soluble A β oligomers and can thus be used to detect and regulate the soluble A β species in AD.

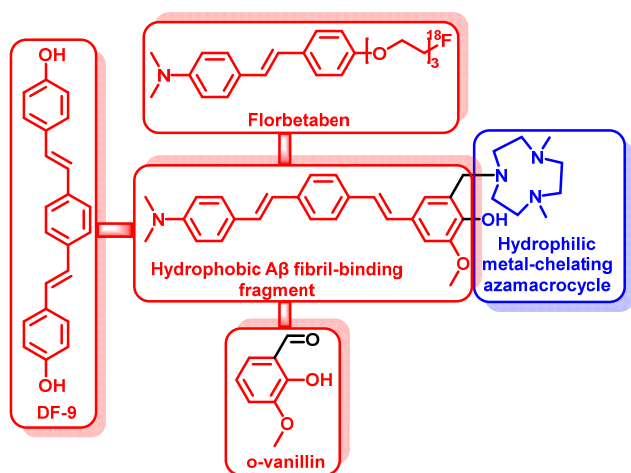
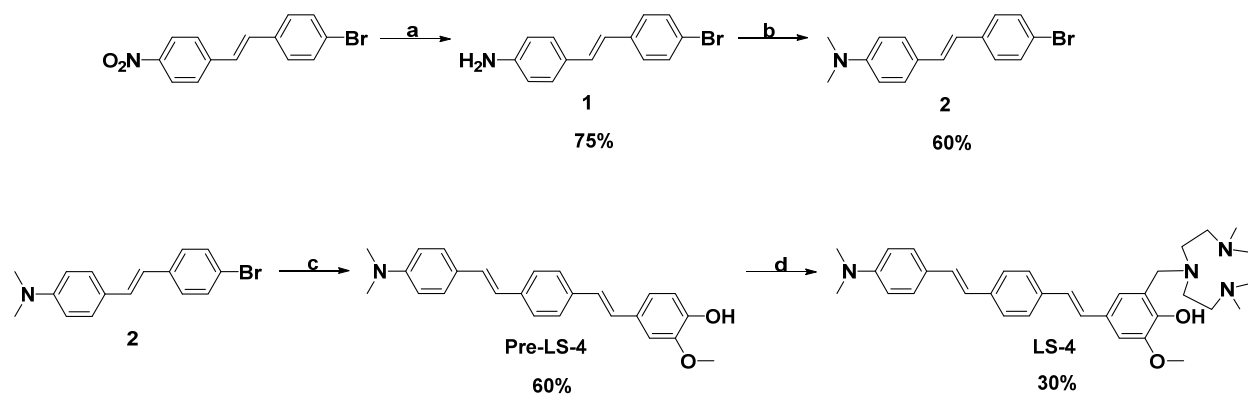


Figure 1. Design strategy and structure of the amphiphilic compound LS-4. The A β fibril-interacting hydrophobic region of LS-4 is shown in red, and the hydrophilic metal-chelating azamacrocycle is shown in blue.

Results and discussion

Synthesis of LS-4 and Pre-LS-4

Recent reports focusing on the soluble A β oligomer structures have shown that the soluble A β aggregates possess an amphiphilic property, including hydrophobic cores and water-soluble hydrophilic regions.⁴³⁻⁴⁵ This type of structure makes the soluble A β oligomers bind to cell membranes and generate pores and channel-like structures that disrupt the neuron cell membrane integrity.⁴⁶⁻⁵⁰ Thus, attaching hydrophilic moieties to the hydrophobic A β fibril-binding fragment can be an effective strategy to design small molecules to probe the soluble A β oligomers, since such amphiphilic molecule can interact with both hydrophobic regions as well as the hydrophilic residues of the soluble A β oligomers. Based on this strategy, the amphiphilic compound LS-4 contains a hydrophilic azamacrocycle, 2,4-dimethyl-1,4,7-triazacyclononane (Me₂HTACN), and a hydrophobic distyryl stilbene derivative known to exhibit high binding affinity for the A β species.⁵¹⁻⁵² The novel asymmetric distyryl stilbene derivative contains fragments resembling the FDA-approved PET imaging agents for AD, fluorbetaben, the symmetric distyrylbenzene structure of compound DF-9 and the related methoxy-X04 – which have been widely used in detecting amyloid plaques,^{15, 53-54} as well as the 2-methoxy-phenol fragment reminiscent of o-vanillin that was shown to inhibit the formation of A β oligomers and also exhibits appreciable antioxidant ability.⁵⁵ Notably, a similar type of asymmetric distyryl structure has been used for membrane potential sensor development,⁵⁶ yet it has never been utilized for binding or detecting A β species in AD. The synthesis of LS-4 employs a Heck reaction to generate the Pre-LS-4 compound first,⁵⁷ followed by the Mannich reaction with paraformaldehyde and the Me₂HTACN azamacrocycle fragment to yield LS-4 (Scheme 1).



Scheme 1 Synthesis of Pre-LS-4 and LS-4. (a) SnCl_2 , conc. HCl , EtOH , reflux, 3h; (b) $(\text{CH}_2\text{O})_n$, NaBH_3CN , CH_3COOH , room temperature, overnight; (c) 2-methoxy-4-vinylphenol, $\text{Pd}(\text{OAc})_2$, triethanolamine, $100\text{ }^\circ\text{C}$, 24 h; (d) Me_2HTACN , $(\text{CH}_2\text{O})_n$, MeCN , reflux, 24 h.

Fluorescence turn-on effect of LS-4 and Pre-LS-4 with $\text{A}\beta$ species

To probe whether introducing the hydrophilic azamacrocycle moiety into the $\text{A}\beta$ fibril-binding fragment can increase the interaction towards various $\text{A}\beta$ species, a fluorescence turn-on assay was performed to evaluate whether LS-4 can interact with both the soluble $\text{A}\beta$ oligomers and insoluble $\text{A}\beta$ aggregates. Interestingly, LS-4 shows a remarkable fluorescence turn-on effect (~ 20 folds) when added to a solution of $\text{A}\beta_{42}$ aggregates (Figure 2a). We have also prepared $\text{A}\beta_{42}$ oligomers according to the procedure reported by Klein⁵⁸ and confirmed their morphology by TEM (Figure S2). Excitingly, in the presence of $\text{A}\beta_{42}$ oligomers, LS-4 shows a more significant 50-fold fluorescence turn-on effect than in the presence of $\text{A}\beta_{42}$ fibrils. Furthermore, we have also checked the fluorescence turn-on effect of Pre-LS-4, which only exhibits a similar small turn-on effect in the presence of either the $\text{A}\beta_4$ oligomers and fibrils (Figure 2b). Thus, this result strongly suggests that the hydrophilic azamacrocycle present in LS-4 enhances the fluorescence turn-on effect in the presence of $\text{A}\beta$ species, especially the soluble $\text{A}\beta_{42}$ oligomers.

The triazamacrocycle moiety is known to act as a strong metal-chelating ligand, including binding to Cu^{2+} ions. Since compound LS-4 should be mono-protonated under normal pH,²⁵⁻³⁰ the Cu^{2+} -LS-4 complex should also be monocationic like the monoprotonated LS-4, and could potentially exhibit similar amyloid binding properties as LS-4. As a result, we have employed the Cu-LS-4 complex to probe its fluorescence properties when interacting with the $\text{A}\beta_{42}$ oligomers and fibrils. Interestingly, when the Cu-LS-4 complex was added to the $\text{A}\beta_{42}$ oligomers or fibrils solution, it also exhibits similar fluorescence turn-on effects as LS-4 (Figure S3). Overall, the fluorescence turn-on results clearly indicate that improving the hydrophilicity of the compound may significantly enhance the binding affinity towards $\text{A}\beta$ oligomers and fibrils.

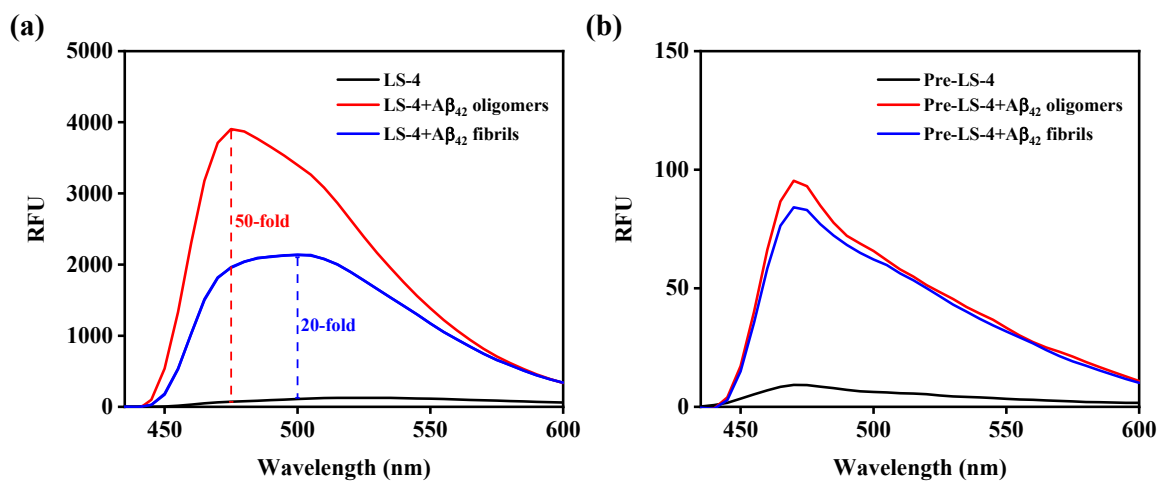


Figure 2. Fluorescence turn-on effects of LS-4 and Pre-LS-4 with $\text{A}\beta_{42}$ oligomers and fibrils. (a) LS-4 (black), $\text{A}\beta_{42}$ oligomer + LS-4 (red) and $\text{A}\beta_{42}$ fibrils + LS-4 (blue); (b) Pre-LS-4 (black), $\text{A}\beta_{42}$ oligomer + Pre-LS-4 (red) and $\text{A}\beta_{42}$ fibrils + Pre-LS-4 (blue). $[\text{A}\beta_{42}] = 25 \mu\text{M}$, $[\text{LS-4}] = [\text{Pre-LS-4}] = 5 \mu\text{M}$, excitation wavelength = 380 nm in pH = 7.4 PBS buffer.

The binding affinity LS-4 and Pre-LS-4 to $\text{A}\beta_{42}$ oligomers and fibrils

To explore further the binding affinity towards A β ₄₂ species, we used different A β ₄₂ species and direct-binding fluorescent assays to measure the K_d values for the developed compounds. Excitingly, LS-4 displays nanomolar affinity for the A β ₄₂ oligomers ($K_d = 50 \pm 9$ nM) and fibrils ($K_d = 58 \pm 15$ nM), indicating that the developed compounds not only bind tightly to the amyloid fibrils, but also to the soluble A β ₄₂ oligomers (Figure 3). However, in the absence of the hydrophilic azamacrocycle fragment, the binding affinity of Pre-LS-4 towards the amyloid species dramatically decreased to 9-10 μ M (Figure S4), strongly suggesting that the hydrophilic moiety plays a significant role in binding to the A β ₄₂ peptides.

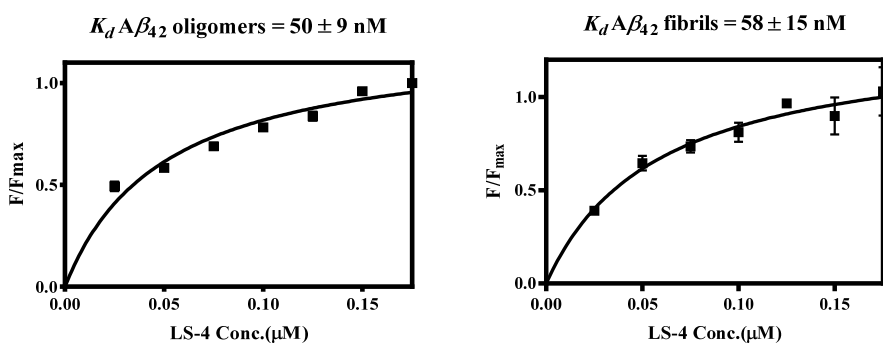


Figure 3. Direct binding constant measurements of LS-4 with A β ₄₂ oligomers (left) and fibrils (right).

Monitoring of the kinetics of A β ₄₂ aggregation

Following the fluorescence turn-on effect studies, the sensing effect of LS-4 during A β ₄₂ aggregation was investigated. Herein, the on-pathway aggregation conditions were employed for the growth of fibrils,⁵⁸ and the whole aggregation process was monitored by ThT. At each selected time point, an aliquot of LS-4 was added to the A β ₄₂ species solution followed by the fluorescence measurement. Interestingly, the fluorescence intensity increased at the beginning and reached the maximum after \sim 2 h of incubation and then decreased dramatically during the following 48 h

incubation period (Figure 4). These observed changes in the fluorescence intensity suggests that LS-4 detects the on-pathway $A\beta_{42}$ oligomers, where the fluorescence signal increases as the monomeric $A\beta_{42}$ aggregates into oligomers, and then decreases as $A\beta_{42}$ fibrils are formed in solution. We have also performed the same kinetics studies to evaluate the $A\beta_{42}$ species-sensing ability for Pre-LS-4, however in this case the fluorescence signal decreased significantly in the first 1 hr and then reached a plateau during the extended incubation time, suggesting that Pre-LS-4 does not follow the same behaviour to detect $A\beta_{42}$ oligomers as LS-4 and also show limited $A\beta$ fibril binding turn-on fluorescence, further proving the importance of the hydrophilic azamacrocycle for binding to the soluble $A\beta_{42}$ oligomers (Figure S5a). Moreover, the $A\beta$ aggregation process was also monitored with the Cu-LS-4 complex, which interestingly shows a similar trend as LS-4 when tracking the $A\beta_{42}$ aggregation process (Figure S5b). The fluorescence intensity increases in line with the formation of the $A\beta_{42}$ oligomers but decreases as the $A\beta_{42}$ fibrils are formed in solution, indicating the Cu-LS-4 complex also has the capacity to detect the soluble $A\beta_{42}$ oligomers, and this property could be used for ^{64}Cu PET imaging applications (see below).

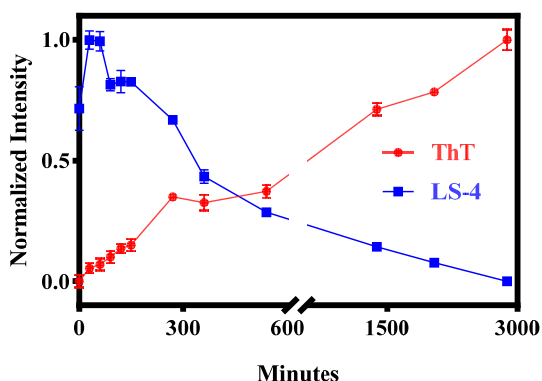


Figure 4. Monitoring of the aggregation process of $A\beta_{42}$ at different time points with LS-4 (blue) and ThT (red). The fluorescence intensities of ThT ($\lambda_{\text{ex}} = 435 \text{ nm}$), LS-4 ($\lambda_{\text{ex}} = 380 \text{ nm}$) were recorded at 485 nm

and 470 nm, respectively. Conditions: $[A\beta_{42}] = 25 \mu\text{M}$, $[LS-4] = 5 \mu\text{M}$. The peptides were incubated in pH = 7.4 PBS buffer at 37 °C with shaking at 1000 rpm for 48 hours.

Fluorescence staining of 5xFAD mouse brain sections

To investigate further the selective staining of the LS-4 and Pre-LS-4 toward various A β species, their intrinsic fluorescence properties were tested in *ex vivo* studies. The brain sections from 7-month old 5xFAD transgenic mice that rapidly develop severe amyloid pathology⁵⁹ were stained with LS-4, and sequentially stained with Congo Red, which is a well-known fluorescent dye,⁶⁰ or immunostained with the HJ3.4 antibody, which can bind to all A β species,⁶¹ or with an A β oligomer-specific monoclonal antibody (OMAB), which could specifically bind to A β oligomers.

⁶² When the 5xFAD mouse brain sections were stained with LS-4, a strong fluorescence signal was detected (Figure 5, left panels), which an excellent colocalization with the immunofluorescence of OMAB (Pearson's correlation coefficients = 0.89). For the brain sections immunostained with HJ3.4, the colocalization of the two set of images is not as excellent as OMAB (Pearson's correlation coefficients = 0.78), probably due to the fact that the HJ3.4 antibody can bind to a wide range of A β species. These results indicate that LS-4 could selectively probe the A β oligomers and fibrils in AD brain sections. The brain sections were also treated with Pre-LS-4 to probe its A β -binding properties, and the fluorescence images show that the colocalization between the compound and HJ3.4 antibody is much lower than LS-4 (Figure S6). This result also suggests that the TACN azamacrocycle is significantly important for A β binding, which is highly consistent with the *in vitro* fluorescence turn-on studies. The brain sections from 5xFAD mice with different ages at early (3-month old), middle (7-month old) and late stage (11-month old) were also used to perform the staining studies. The images show that LS-4 can efficiently and clearly label amyloid

plaques for all 3 different ages. However, for Pre-LS-4, the fluorescence signal of amyloid plaques is extremely low under the same conditions as LS-4 (Figure S7). To explore further the affinity of the Cu^{2+} -LS-4 complex towards amyloid plaques, the 5xFAD brain sections were sequentially stained with the Cu^{2+} -LS-4 complex followed by Congo Red, HJ3.4 antibody staining, or OMAB antibody staining. The fluorescence images show that the Cu^{2+} -LS-4 complex has fairly good colocalization with Congo red, HJ3.4, and OMAB staining, indicating that the Cu-complex also exhibits the ability to selectively bind and probe $\text{A}\beta$ species *ex vivo* similar as LS-4 (Figure S8). This also lends support to the possibility of using ^{64}Cu -LS-4 as a ^{64}Cu PET imaging agent for amyloid plaques in AD (see below).

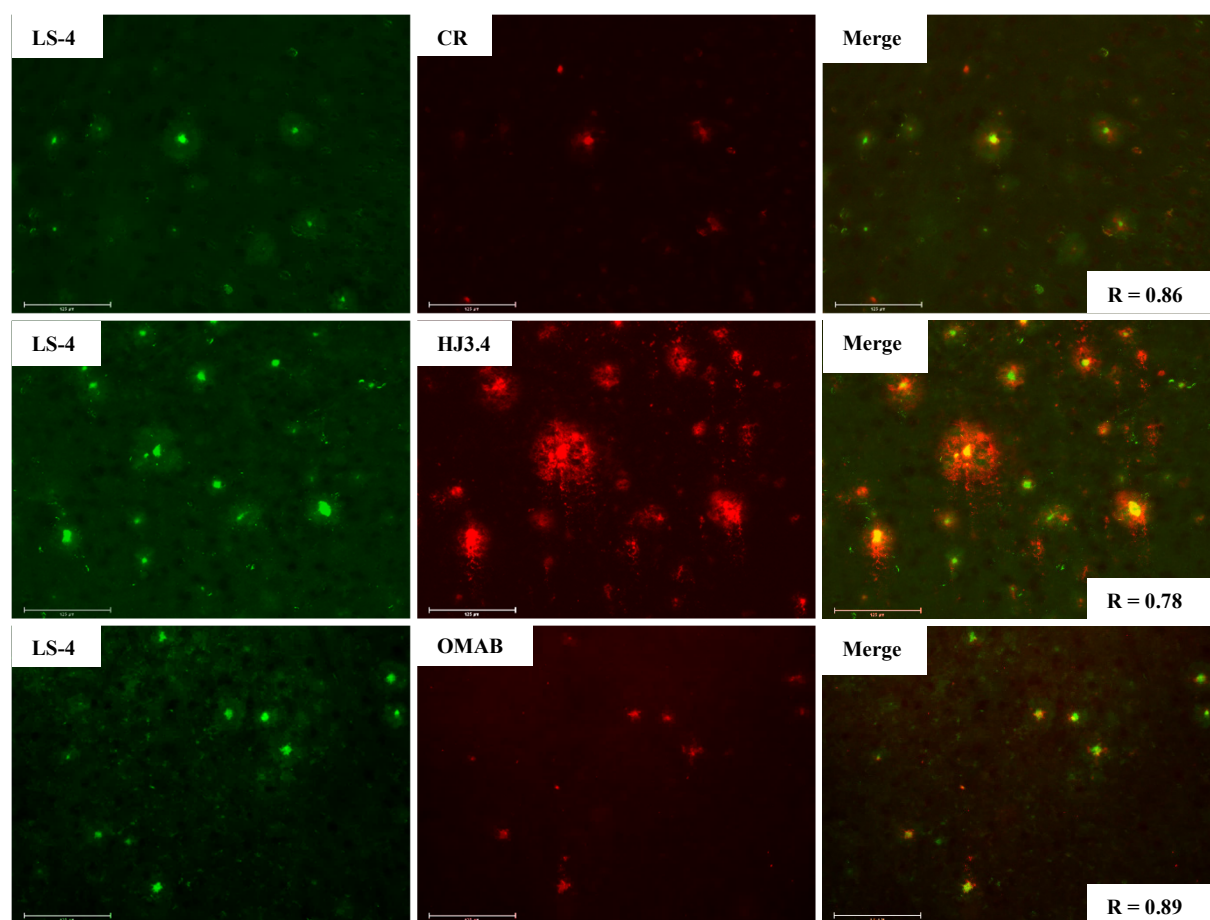


Figure 5. Fluorescence microscopy images of 5xFAD mice brain sections incubated with LS-4 (left panels), Congo Red, HJ3.4, or OMAB (middle panels), and merged images (right panels). [LS-4] = 25 μ M, [Congo Red] = 5 μ M, [HJ3.4] = 1 μ g/ml, [OMAB] = 2 μ g/ml. LS-4 has significant colocalization with the amyloid species stained with Congo Red, HJ3.4 antibody, or OMAB. Scale bar: 125 μ m.

Trolox equivalent antioxidant capacity assay

To explore the antioxidant capability of the developed compounds, Trolox-Equivalent Antioxidant Capacity (TEAC) assays were employed to evaluate the antioxidant ability of the phenolic moiety from Pre-LS-4 and LS-4. The TEAC assay has been widely used for measuring the antioxidant activity of foods by monitoring the UV-Vis to follow the scavenging of the ABTS^{•+} radical cation.⁶³ Trolox, a water-soluble analogue of vitamin E, has strong antioxidant properties and was used as a standard.⁶⁴ In addition, Pre-LS-4 and LS-4 were also compared with glutathione, which has an appreciable antioxidant ability and plays a fundamental role in detoxification of reactive oxygen species (ROS), which play a detrimental role in many diseases including AD.⁶⁵ Interestingly, both Pre-LS-4 and LS-4 show very good antioxidant capacity compared to Trolox (Figure 6), indicating that the developed compounds can quench the radical species efficiently and protect the cells from oxidative stress – with or without the presence of the azamacrocyclic fragment, likely due to the electron-rich 2-methoxyphenol moiety.

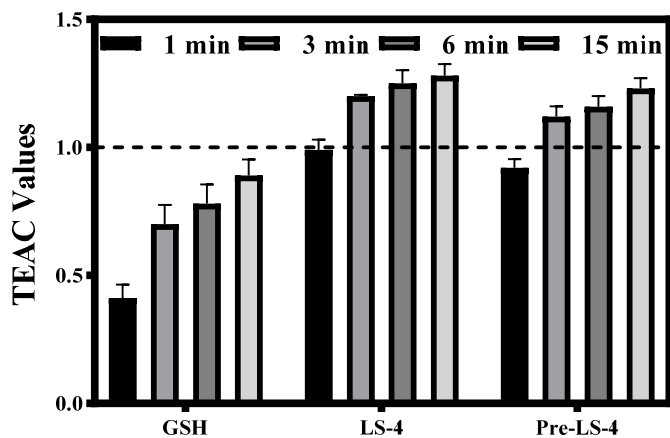


Figure 6. Trolox-equivalent antioxidant capacity (TEAC) values at 1, 3, 6, and 15 min for Trolox, glutathione, LS-4, and Pre-LS-4. The TEAC values of glutathione, LS-4 and Pre-LS-4 are normalized to the antioxidant activity of Trolox (shown by the dashed line). Each experiment was completed in triplicate and the error bars represent standard deviation (n=5) for the average TEAC values.

Cu²⁺-induced ascorbate consumption assay

It is known that the Cu²⁺-Aβ₄₂ species can promote the formation of ROS that have deleterious effect in AD.⁶⁶ Herein, we performed an ascorbate consumption assay to evaluate the ability of LS-4 to suppress the Cu²⁺-ascorbate redox cycling. In the absence of LS-4, the consumption of ascorbate in the presence of Cu²⁺ is rapid (Figure 7a, black); however, if Cu²⁺ is premixed with 2 eq of LS-4, the ascorbate consumption is virtually eliminated (Figure 7a, red), indicating that LS-4 can bind tightly to Cu²⁺ and mitigate the redox cycling. Furthermore, adding LS-4 into the Cu²⁺-ascorbate solution, the consumption of ascorbate can be arrested immediately and significantly (Figure 7a, blue), showing that the LS-4 can efficiently regulate the redox process. We also investigated ascorbate consumption in the presence of Aβ₄₂, mimicking conditions that are more relevant to the conditions in AD. Compared with the Cu²⁺-Aβ₄₂ species, addition of 2 eq LS-4

leads to a significant inhibition of ascorbate consumption (Figure 7b), suggesting that LS-4 can strongly bind to Cu^{2+} and silent the Cu^{2+} redox cycle in the presence of $\text{A}\beta_{42}$ species. Moreover, LS-4 can also shut down the consumption of ascorbate rapidly. These results show that the LS-4 can efficiently chelate the Cu^{2+} to prevent the reduction by ascorbate, even in the presence of the $\text{A}\beta$ species, inhibiting the formation of ROS species upon redox cycling. By comparison, upon addition of Pre-LS-4, the rate of consumption of ascorbate is similar as for Cu^{2+} -ascorbate redox reaction (Figure S9), suggesting that the compound cannot readily regulate the consumption of ascorbate since it is missing the metal-chelating azamacrocycle fragment.

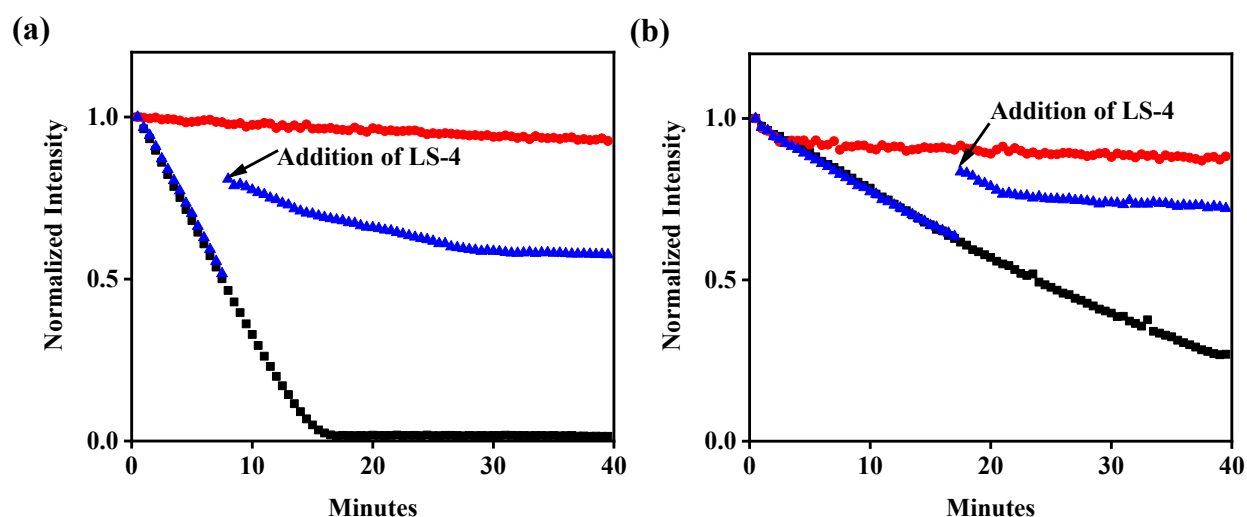


Figure 7. Kinetics of ascorbate consumption monitored by UV-visible spectroscopy at 265 nm. (a) Cu^{2+} + ascorbate (black), Cu^{2+} + LS-4 + ascorbate (red), Cu^{2+} + ascorbate + LS-4 (blue); (b) Cu^{2+} + $\text{A}\beta_{42}$ + ascorbate (black), Cu^{2+} + $\text{A}\beta_{42}$ + LS-4 + ascorbate (red), Cu^{2+} + $\text{A}\beta_{42}$ + ascorbate + LS-4 (blue). $[\text{Cu}^{2+}] = 10 \mu\text{M}$, $[\text{A}\beta_{42}] = 12 \mu\text{M}$, $[\text{LS-4}] = 24 \mu\text{M}$, $[\text{ascorbate}] = 100 \mu\text{M}$.

Attenuation of copper-induced A β ₄₂ cytotoxicity by LS-4

Since the Cu²⁺-A β ₄₂ species were shown to be neurotoxic,⁶⁷ it is important to develop novel metal-chelating compounds that can control the Cu²⁺-induced A β ₄₂ cytotoxicity. In this respect, we investigated the effect of LS-4 to alleviate the neurotoxicity of Cu-A β ₄₂ in N2a cells by using the Alamar blue cell viability assay.⁶⁸ Interestingly, in the presence of A β ₄₂ and Cu²⁺, LS-4 can rescue the N2a cells and alleviate the neurotoxicity of Cu²⁺-mediated A β ₄₂ species (Figure S11). Overall, the above antioxidant, ROS and cytotoxicity studies suggests that LS-4 could be useful as a modulator of the oxidative stress and ROS formulation and as a potential therapeutic agent for AD.

Treatment of 5xFAD transgenic mice

The blood-brain barrier (BBB) permeability of lead compounds is highly crucial for any *in vivo* applications. In order for the compounds to penetrate the BBB, their lipophilicity should be within the 0.9-2.5 range.⁶⁹ Since we introduced a hydrophilic azamacrocycle fragment into the structure of LS-4, it is important to confirm that LS-4 still possesses enough lipophilicity to cross the BBB. The lipophilicity of the compounds was determined by measuring the octanol-PBS partition coefficients logD. While for Pre-LS-4 a higher log D value of 1.22 ± 0.04 was found, LS-4 exhibits a logD value of 0.98 ± 0.13 , suggesting that LS-4 should be able to cross the BBB. To confirm this, 7-month old 5xFAD mice were daily administered for 10 days with LS-4 (1 mg/kg of body weight) via intraperitoneal injection. Excitingly, the brain sections from LS-4-treated mice displayed remarkably strong fluorescence of the accumulated LS-4 staining the A β species (Figure 8, left panel). Immunohistochemical staining was then employed to confirm the A β -binding specificity of LS-4. First, the LS4-treated 5xFAD brain sections were stained with Congo red, which is known to stain the mature amyloid fibrils, and the colocalization images show that LS-4

can label more types of A β species than Congo Red (Figure 8, top panel). Then, the brain sections were also immunostained with the pan-A β antibody HJ3.4, which can recognize a wide range of A β species, and the fluorescence images show that the HJ3.4-stained regions are broader than the LS-4-stained regions, although an appreciable colocalization was observed (Figure 8, middle panel). Hereafter, brain sections were treated with an A β oligomer-specific monoclonal antibody (OMAB) that can stain the A β oligomers specifically. The images demonstrated that LS-4 exhibited excellent colocalization with the OMAB antibody, supporting that LS-4 has the ability to stain the A β oligomers (Figure 8, bottom panel). Consequently, all these data substantiate that the compound can efficiently penetrate the BBB and stain both A β oligomers and fibrils, which is consistent with the *ex vivo* studies.

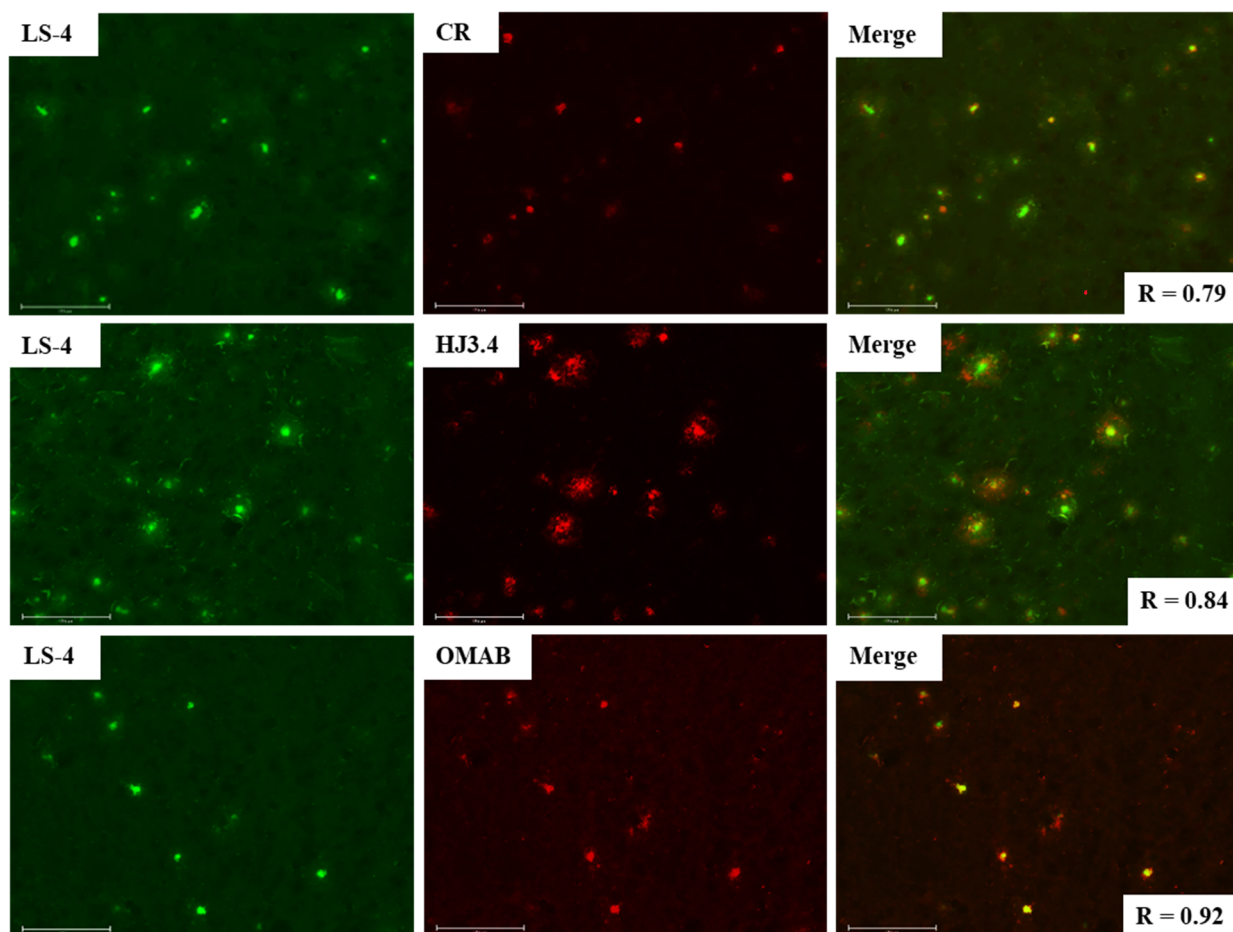


Figure 8. Representative fluorescence microscopy images of brain sections from LS-4 administrated 7-month 5xFAD mice for 10 days. The brain sections were immunostained with Congo Red, HJ3.4 and OMAB antibody. [Congo Red] = 5 μ M, [HJ3.4] = 1 μ g/ml, [OMAB] = 2 μ g/ml. Scale bar: 125 μ m. The *in vivo* LS-4 has significant colocalization with the amyloid species immunostained with Congo Red (Pearson's $r = 0.79$), HJ3.4 (Pearson's $r = 0.84$), OMAB (Pearson's $r = 0.92$).

In vivo regulation of A β species

To evaluate the *in vivo* therapeutic efficacy of LS-4, we have administered the LS-4 compound daily to 5xFAD mice (1 mg/kg of body weight) via intraperitoneal injection for 30 days. Since the amyloid plaques began to deposit in the deep cortex and subiculum of 5xFAD mice at 2 months of

age,⁵⁹ 3-month-old 5xFAD mice were selected that contain multiple forms of A β species, including A β monomers, soluble A β oligomers, intraneuronal A β aggregates, and amyloid plaques.⁷⁰ Other 5xFAD mice were treated with the vehicle (1% DMSO in PBS) daily, as a control group. After 30 days, the brains were harvested and 50 μ m thick brain sections were obtained. For the quantitative analysis of all amyloid aggregates, immunostaining with the CF594-HJ3.4 antibody was performed for the treated 5xFAD mice brain sections. We have quantified the amyloid plaques in the brain sections by analyzing the area of the antibody-stained plaques of 8 brain sections per mouse that were sliced from uniformly distributed locations between the frontal lobe and the occipital lobe. For each brain section, 5 regions throughout the cortex area were randomly selected and the areas of antibody-stained amyloid plaques were quantified. The fluorescence images show that the areas of HJ3.4-labeled amyloid aggregates were significantly reduced by ca. 60% in the LS-4-treated brain sections vs. the vehicle-treated 5xFAD mice brain sections (Figure 9b). To confirm the ability that the LS-4 can modulate the A β aggregation process *in vivo*, the total amount of cerebral A β peptides were quantified by using A β enzyme-linked immunosorbent assay (ELISA). Importantly, the amount of PBS-soluble and guanidine-soluble A β ₄₂ was reduced dramatically by ca. 66 % and 72%, respectively, upon treatment with LS-4 vs. vehicle (Figure 9c). In addition, the levels of guanidine-soluble A β ₄₀ were also drastically decreased by ca. 76% (Figure S12). Overall, these results indicate that LS-4 is able to significantly delay and mitigate the aggregation of A β species in 5xFAD mice via strong binding to both A β oligomers and fibrils.

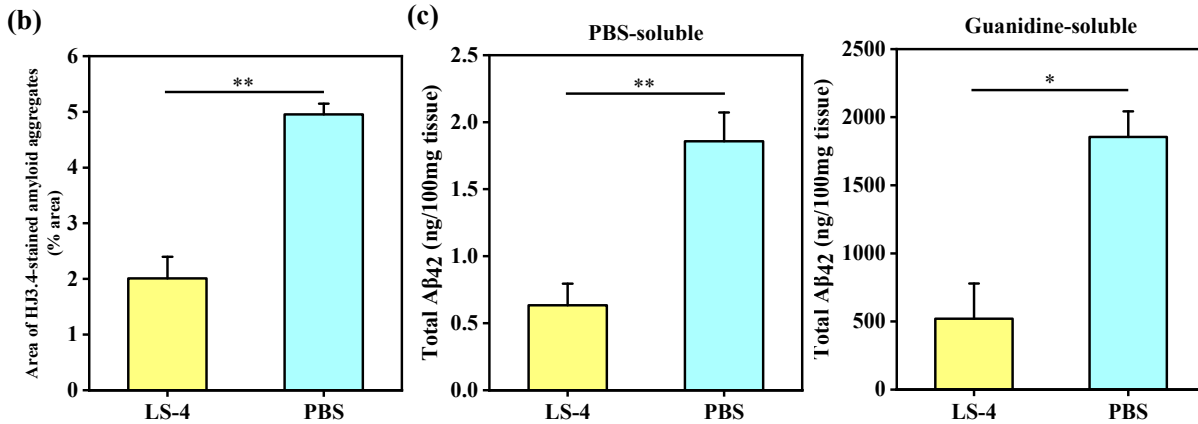
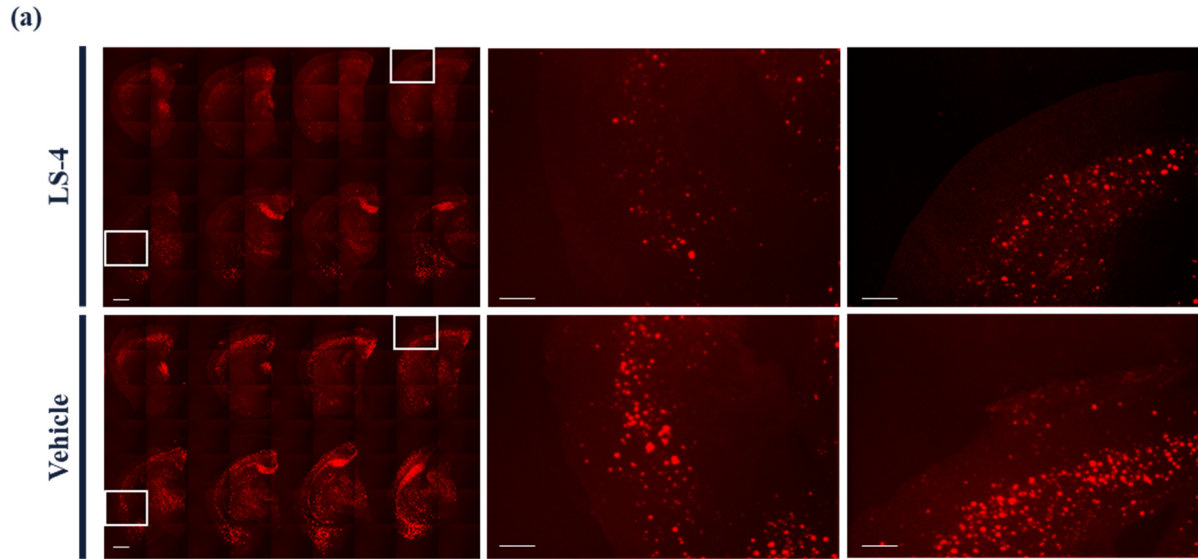


Figure 9. Reduction of cerebral amyloid pathology by LS-4 in the 5xFAD mice. The brain tissues were collected from the 3-months-old 5xFAD mice after 30 days i.p. injections of LS-4 or vehicle. (a) Representative fluorescence microscopy images of the CF594-HJ3.4 antibody-stained brain sections from 5xFAD mice treated with LS-4 and vehicle. Scale bar = 500 μ m. (b) Total area of HJ3.4-staining amyloid plaques in the brain sections from 5xFAD mouse treated with LS-4 and vehicle. The area of antibody-stained amyloid plaques was selected from 8 brain sections per mice. For each brain section, five random area across cortex regions were chosen. Error bars represent the standard deviation (LS-4 treated mice, n = 4, vehicle-treated mice, n=3), and the statistical analysis was evaluated according to one-way ANOVA (** p < 0.01) (c) The bars indicate the amount of PBS-soluble (left) and Guanidine-soluble A β ₄₂ (right) levels

from brain tissues. With the treatment of LS-4, the amount of A β ₄₂ species were dramatically reduced by ca. 66% and 72% in PBS- and Guanidine-soluble brain homogenates. Error bars represent standard deviations (LS-4 treated mice, n = 5, vehicle-treated mice, n = 3), and the statistical analysis was evaluated according to one-way ANOVA (** p < 0.01, * p < 0.05).

Attenuation of A β -induced p-tau aggregation and neuroinflammation in 5xFAD mice

Recently, several clinical trials focusing on A β -targeting therapeutics have failed,⁷¹⁻⁷² and the amyloid cascade hypothesis is being re-evaluated and new therapeutics are now focusing on additional pathologies such as p-tau aggregation and neuroinflammation. Therefore, it has been proposed that therapeutic agents targeting the tau pathology and neuroinflammation could be more effective than A β -targeting therapeutics, since tau hyperphosphorylation and p-tau aggregates are more closely correlated to the cognitive and clinical symptoms of AD than the amyloid plaques formation, although the amyloid plaques have been shown to facilitate the initial p-tau aggregation surrounding the amyloid plaques and the spread of formation of the intracellular neurofibrillary tangles (NFT).⁷³⁻⁷⁴ Therefore, we investigated the effect of LS-4 on the aggregation of p-tau protein and the activation of microglia as a neuroinflammatory response. Although the 5xFAD mouse model does not exhibit an obvious tau pathology, a substantial amount of extracellular p-tau aggregates are still observed in the cortex and hippocampus regions of the 5xFAD mice.⁷⁵ Therefore, a fluorescent labeled AT8 antibody, which can specifically recognize p-tau aggregates, was employed to immunostain the p-tau aggregates surrounding the amyloid plaques and to quantify the amount of the p-tau aggregates. Excitingly, we found that the amount of p-tau aggregates around amyloid plaques were significantly decreased by ~47% in the LS-4-treated vs vehicle-treated 5xFAD mice (Figures 10b and S13). This result is exciting, since recent amyloid-targeting immunotherapy showed the A β specific antibodies efficiently reduce the A β deposition,

yet they have no effect on p-tau aggregation *in vivo*.⁷⁶⁻⁷⁹ Although the role of A β species in the initial p-tau aggregation and the formation in intracellular NFT and their neurotoxicity is still not clear, these results suggest that LS-4 decreases the amount of p-tau aggregates surrounding the amyloid plaques.

Since it was shown that soluble A β oligomers and A β fibrils can bind to and activate the microglial cells via cell-surface receptors to initiate a neuroinflammatory response, inducing neuron injury in AD, it is important to evaluate the level of activated microglia cells in AD mice.⁸⁰⁻
⁸¹ Therefore, the CF594-labeled Anti-Iba1 antibody was employed to detect via immunofluorescence staining the Iba1 protein, which is specifically expressed in microglia cells. Strikingly, the expression of Iba1 was dramatically decreased near the amyloid plaques upon the treatment of LS-4 (Figure 10a), with the fluorescence intensity of Iba1 antibody being reduced by ~52% vs. the vehicle-treated 5xFAD mice (Figures 10c and S14), indicating LS-4 could suppress the overactivation of microglia cells to alleviate the neuroinflammation in 5xFAD mice. These results further support that LS-4 can regulate the A β aggregation process and alleviate the A β -induced neurotoxicity, leading to the attenuation of neuroinflammation mediated by the microglia activation near the amyloid plaques.

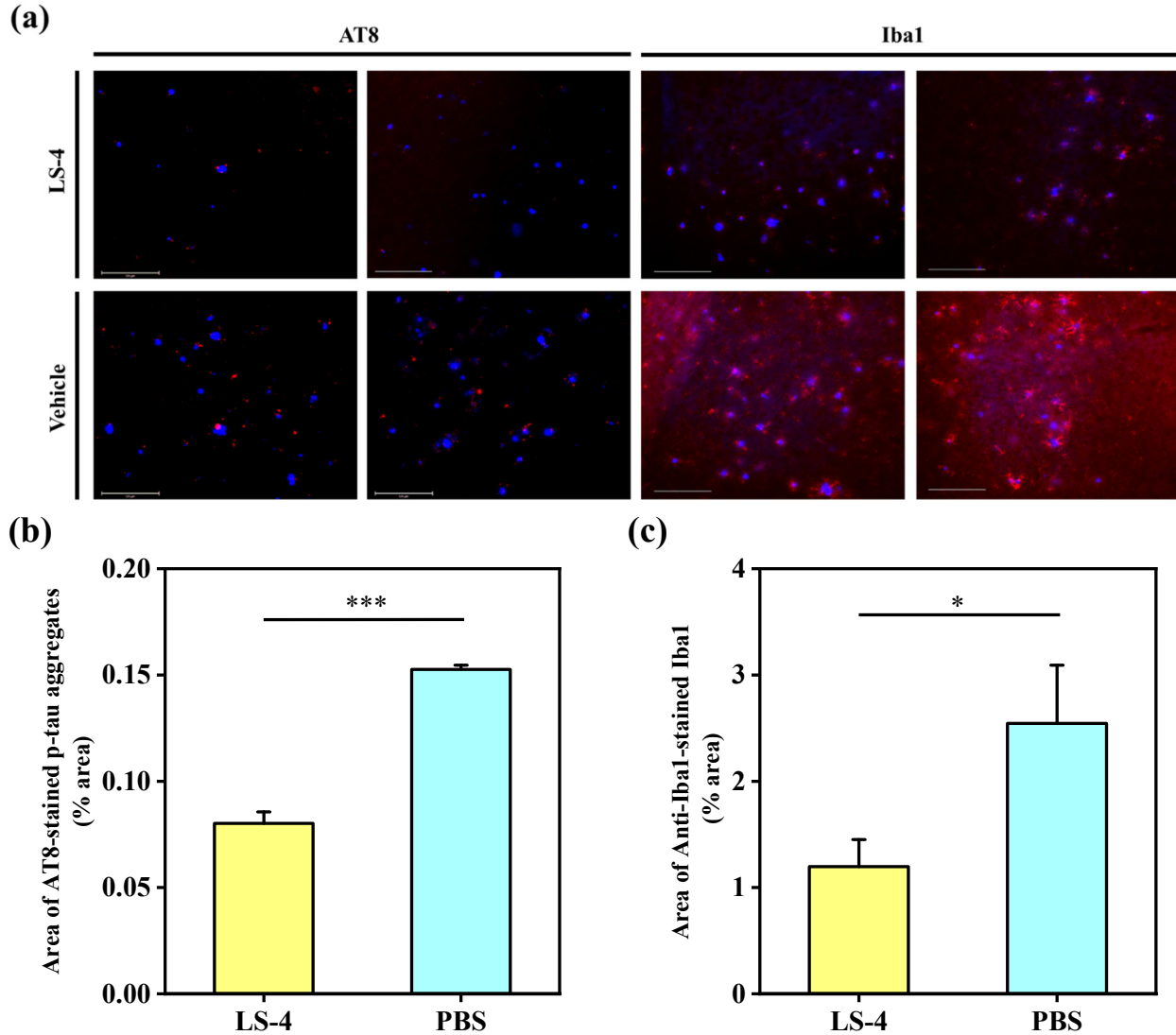


Figure 10. (a) Representative fluorescence microscopy images of the CF594-AT8 and CF594-Iba1 immunostained brain sections from 5xFAD mice treated with LS-4 and vehicle. All fluorescence images are the maximum intensity projection images obtained from 30 Z-sections collected at 1 μ m intervals. Color: red, CF594-Iba1 or CF594-AT8 antibody; blue, ThS. Scale bar: 125 μ m. (b) Quantification of the area of CF594-AT8 immunostained brain sections from 5xFAD mice. All data were obtained from 8 brain sections per mice. For each brain section, four random area across cortex regions were chosen. Error bars represent the standard deviation (LS-4 treated mice, n = 4, vehicle-treated mice, n=3), and the statistical analysis was evaluated according to one-way ANOVA (***) $p < 0.001$. (c) Quantification of the area of CF594-Iba1 immunostained brain sections from 5xFAD mice. All data were obtained from 8 brain sections per mice.

For each brain section, four random area across cortex region were chosen. Error bars represent the standard deviation (LS-4 treated mice, n = 4, vehicle-treated mice, n=3), and the statistical analysis was evaluated according to one-way ANOVA (*p < 0.05).

Docking studies and MD simulations

To gain molecular insight into the nature of the interactions of LS-4 with the A β aggregates, molecular docking and MD simulations⁸²⁻⁸³ were performed to characterize the binding of LS-4 to both soluble A β oligomers and A β fibrils. First, LS-4 and Pre-LS-4 were docked onto the NMR-resolved A β fibril structure (PDB ID: 2LMN),⁸⁴ as well as onto the recently reported NMR/MD structure of the lipid membrane-bound A β ₄₂ octamer (PDB ID: 6RHY).⁴⁴ Interestingly, analysis of large ensembles of tens of thousands of poses of the two compounds docked onto the two protein structures show that LS-4 mainly occupies the two ends of the fibril in a partially inserted configuration (Figures 11a, S15a), whereas Pre-LS-4 can be evenly distributed in the entire fibril cavity (Figures 11b, S15b). In contrast to the A β fibril, there is almost no difference in the occupancy map of LS-4 and Pre-LS-4 for the A β oligomer (Figure S16). MD simulations were performed for the most energetically favorable poses, followed by interaction energy calculations of the two compounds and the two protein structures. Although the van der Waals interaction energies between Pre-LS-4 and LS-4 with the A β fibril are very similar, the presence of the TACN azamacrocyclic in LS-4 increases the electrostatic coupling originating from the interactions between the amine groups and ASP23 of the A β peptide (Figure 11c), while multiple nonpolar amino acids such as PHE19, ALA21, ALA30 and ILE32 are surrounding the phenyl-vinylene fragments for both LS-4 and Pre-LS-4. Moreover, similar to the LS-4-A β fibril interactions, LS-4 provides stronger electrostatic interactions thano Pre-LS-4 with the A β oligomer embedded into

the lipid bilayer (Figure S17). In this case, membrane curvature occurs as a result of hydrophilic side chains attracting water and lipid head groups, forming water pores and causing nearby lipids to curve along the water pores. Although the planar portion of LS-4 and Pre-LS-4 both intercalate in between the octamer leaflets, interaction energy analysis finds that the TACN azamacrocyclic in LS-4 experiences electrostatic stabilization via curved, neighboring lipid head groups (Figure S17a). This effect allows LS-4 to make favorable electrostatic interactions with the solvent and lipid head groups, which is completely absent for Pre-LS-4 (Figure S17b, c), further supporting the amphiphilic nature of LS-4. Overall, these detailed computational studies strongly support our hypothesis that such amphiphilic aromatic-azamacrocyclic compounds have the potential of exhibiting increased affinity for the soluble A β oligomers, as well as their ability to likely interact *in vivo* with the A β aggregates and lipid membranes and thus control their neurotoxicity.

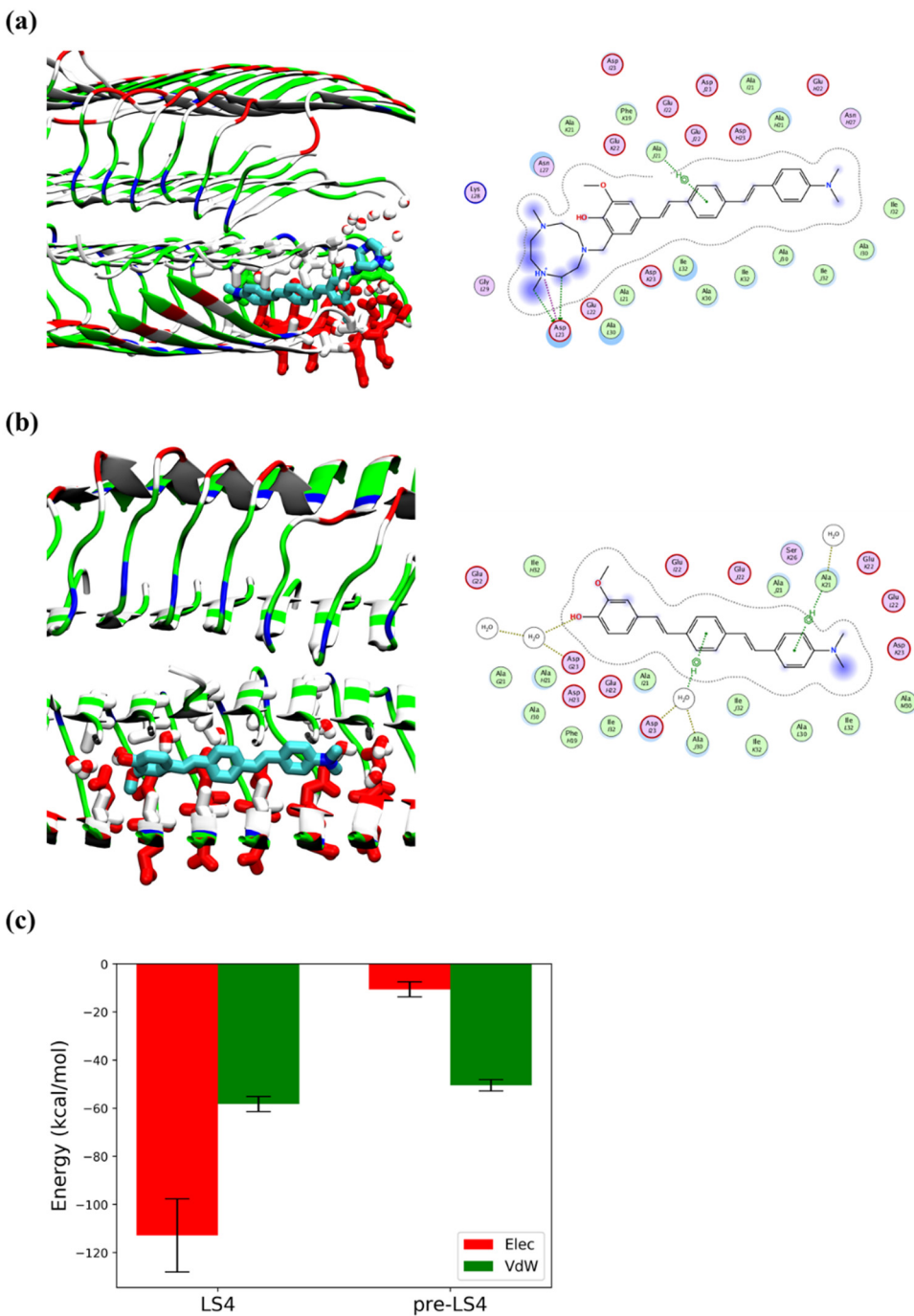


Figure 11. Detailed interactions of LS-4 and Pre-LS-4 docked to the A β fibril after 100 ns simulations. Compounds are shown by licorice representation colored by atoms (C: cyan, N: blue, O: red), the water molecules and amino acid side chains within 3 Å of the compounds are displayed by licorice representation. Acidic, basic, polar and nonpolar amino acid residues are shown in red, blue, green and white colors,

respectively, water molecules are colored by atoms (O: red, H: white). For 2D compound-protein interaction patterns, the close-by protein residues and solvent molecules are shown in proximity around the compound. The compound is annotated with a proximity contour and solvent exposure while the protein residues are also annotated by solvent exposure. The green dotted lines with arrows represent H-bonding with protein side chains, whereas the purple dotted line highlights the presence of a salt bridge. (a) Interaction of LS-4 with the A β fibril, (b) Interaction of Pre-LS-4 with the A β fibril, (c) Electrostatic and van der Waals interaction energies of LS-4 and Pre-LS-4 with A β fibril, averaged over the last 25 ns of the MD simulations.

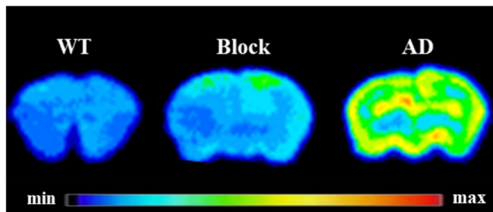
LogD Determination of the ⁶⁴Cu-LS-4 Complex

Numerous studies have reported that A β -targeting bifunctional chelators can be utilized as potential ⁶⁴Cu PET imaging agents for AD.⁸⁵⁻⁸⁹ With the introduction of the hydrophilic metal-chelating azamacrocyclic, the developed amphiphilic compound LS-4 could serve as a bifunctional chelator. Given the promising results from the *ex vivo* studies using the non-radioactive Cu-LS-4 complex, we set out to explore whether the radioactive ⁶⁴Cu-LS-4 complex could be used as a potential PET imaging agent for AD. Firstly, the radiolabeling of LS-4 was performed using ⁶⁴CuCl₂ and following the conditions described in the experimental section. The radio-HPLC trace shows that LS-4 can efficiently chelate ⁶⁴Cu (Figure S18). Since an imaging agent aimed at detecting the A β species for AD diagnosis needs to be able to cross the blood-brain barrier (BBB), the lipophilicity of the ⁶⁴Cu complex was determined by measuring the octanol-PBS partition coefficient logD. The obtained logD value of 1.07 ± 0.13 for the ⁶⁴Cu-LS-4 complex indicates that the compound is sufficiently hydrophobic to cross the BBB.⁶⁹

Ex vivo autoradiography studies

Given promising lipophilicity of the ^{64}Cu -LS-4 complex, *ex vivo* autoradiography studies were performed with 5xFAD mouse brain sections to determine if ^{64}Cu -LS-4 can bind to the amyloid species specifically. The 5xFAD mouse brain sections treated with ^{64}Cu -LS-4 showed a significantly stronger autoradiography intensity than the WT mouse brain sections (Figure 12), and the autoradiography intensity was diminished in the presence of a non-radioactive, $\text{A}\beta$ -binding blocking agent, thus confirming a specific binding to the $\text{A}\beta$ species. Consequently, the autoradiography studies suggest that ^{64}Cu -LS-4 can specifically bind to the amyloid plaques, which is also consistent with the *ex vivo* immunofluorescence brain sections staining with Cu-LS-4 complex, and indicating its ability to detect various $\text{A}\beta$ species *in vivo*.

(a)



(b)

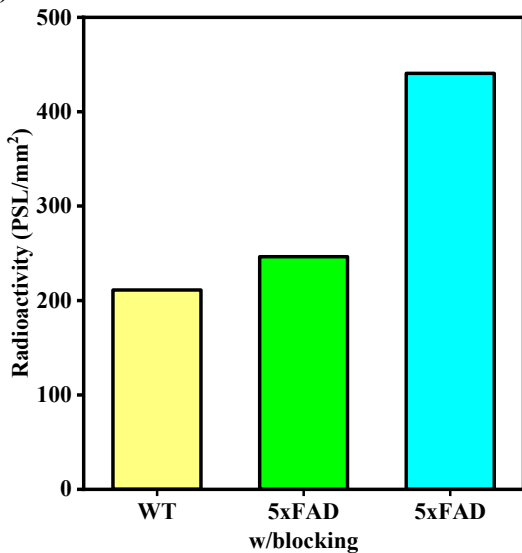


Figure 12. (a) Autoradiography images of brain sections of WT and 5xFAD mice, in the presence or absence of a known A β -specific blocking agent. (b) Quantitative results of autoradiography study of brain sections of WT and AD mice (5xFAD) with the absence and presence with a non-radioactive A β -binding blocking agent.

Biodistribution studies

Inspired by the promising *in vitro* and *ex vivo* studies, we performed *in vivo* biodistribution experiments to explore the pharmacokinetics of ^{64}Cu -LS-4 by using 5xFAD mice and age-matched WT mice. Notably, the ^{64}Cu -LS-4 complex displayed an appreciable brain uptake of 0.75 ± 0.10 %ID/g at 2 min post-injection for the WT mice, which decreased to 0.18 ± 0.02 %ID/g at 1 h, thus indicating that ^{64}Cu -LS-4 can cross the BBB and then is washed out from the brain rapidly for the WT mice. Excitingly, in AD mice the ^{64}Cu -LS-4 complex exhibits a brain uptake 0.79 ± 0.06 %ID/g at 2 min post-injection, and an appreciable brain uptake at 1 h and 4 h (0.39 ± 0.02 %ID/g) is still detected, which is significantly higher than for the WT mice. This is most likely due to the binding of the ^{64}Cu -LS-4 complex to the amyloid plaques in the 5xFAD mouse brains (Figure 13a). *Ex vivo* autoradiography studies of the brain sections performed at each time point confirm that the 5xFAD mouse brains exhibit higher autoradiography intensity than WT mouse brains at both 1 h and 4 h, confirming that ^{64}Cu -LS-4 can penetrate the BBB and label the amyloid species specifically and leading to the delayed washout of ^{64}Cu -LS-4 from the brain. (Figure 13b), Overall, these biodistribution studies suggest that the ^{64}Cu -LS-4 displays the ability to stain the various A β species specifically *in vivo*, and thus could be used as a lead compound for the development of ^{64}Cu PET imaging agents for AD.

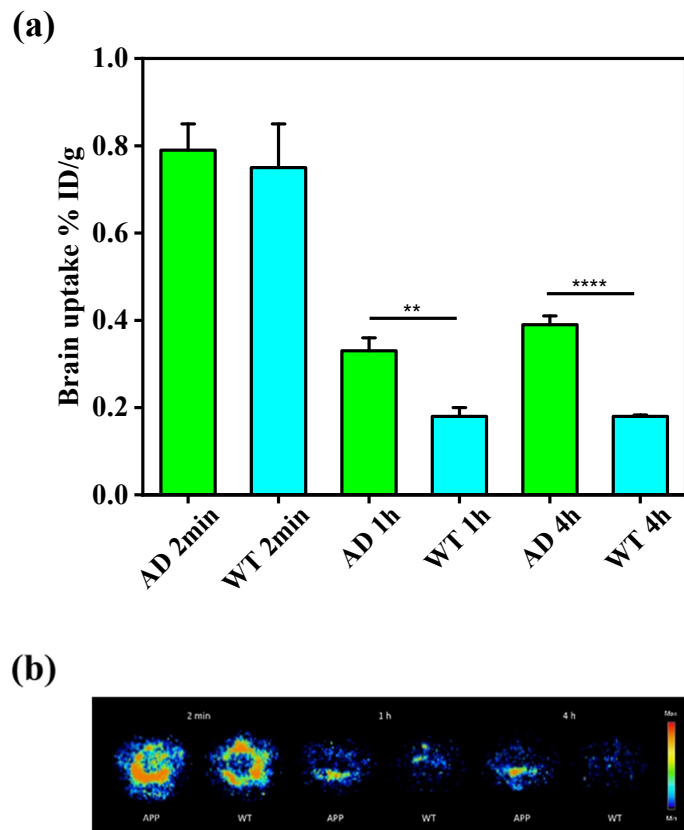


Figure 13. (a) Brain uptake (%ID/g) results from the *in vivo* biodistribution study of ^{64}Cu -LS-4 in 11-month old 5xFAD mice (green) vs. age-matched WT mice (cyan), at 2 min, 1, and 4 h post injection. Error bars represent standard deviations ($n = 3$), and the statistical analysis was evaluated according to one-way ANOVA (** $p < 0.01$, **** $p < 0.0001$). (b) Autoradiography images of brain sections from 5xFAD and WT mice at different time point in biodistribution studies.

Conclusion

Herein, we report the development of a novel amphiphilic compound, LS-4, generated by linking a hydrophobic amyloid fibril-binding fragment with a hydrophilic azamacrocycle that can dramatically increase the binding affinity towards various amyloid β ($\text{A}\beta$) peptide aggregates. The LS-4 compound contains an asymmetric, hydrophobic distyrylbenzene fragment – which has not

been used previously for amyloid-binding studies, and a hydrophilic triazamacrocycle fragment that can interact with the polar residues of the A β species. Excitingly, LS-4 exhibits uncommon fluorescence turn-on and high binding affinity for A β aggregates, especially for soluble A β oligomers. By comparison, the compound Pre-LS-4 – which contains only the hydrophobic conjugated aromatic fragment without the hydrophilic azamacrocycle moiety, exhibits significantly reduced binding affinity for the A β species. Moreover, upon the administration of LS-4 to 5xFAD mice, fluorescence imaging of the LS-4-treated brain sections reveals that LS-4 can readily penetrate the blood-brain-barrier (BBB) and bind to the A β oligomers *in vivo*, as confirmed by immunostaining with an A β oligomer-specific antibody. In addition, the treatment of 5xFAD mice with LS-4 significantly reduces the amount of both amyloid plaques and associated phosphorylated tau (p-tau) aggregates vs. the vehicle-treated 5xFAD mice, while microglia activation is also reduced. Furthermore, MD simulations corroborate the observation that introducing a hydrophilic moiety into the molecular structure can significantly enhance the electrostatic interactions with the polar residues of the A β peptide species. Finally, taking advantage of the strong Cu-chelating property of the azamacrocycle, we performed a series of radioimaging and biodistribution studies that show the ⁶⁴Cu-LS-4 complex binds to the amyloid plaques and can accumulate a significantly larger extent in the 5xFAD mice brains vs. the WT controls. Overall, these *in vitro* and *in vivo* studies illustrate that the novel strategy to employ an amphiphilic molecule containing a hydrophilic fragment attached to a hydrophobic amyloid fibril-binding fragment can increase the binding affinity of these compounds for the soluble A β oligomers and can thus be used to detect and regulate the soluble A β species in AD.

Acknowledgements

This work was supported by the NIH (R01GM114588 to L.M.M.) E.T. was supported by the National Institutes of Health (P41-GM104601) and also acknowledges computing resources provided by Blue Waters at National Center for Supercomputing Applications. We thank the small animal imaging facilities at Washington University School of Medicine for excellent technical assistance and the Isotope Production Group at Washington University for on time weekly production of ^{64}Cu .

Author contributions

L.M.M. conceived the initial idea and supervised the study and the overall manuscript preparation. L.S., H.-J.C., B.E.R., E.T., and L.M.M. designed the *in vitro* and *in vivo* studies. L.S., H.-J.C., and Y.H. carried out the experiments and analyzed the data. S.S. and A.S.A conducted the molecular docking and MD simulation studies. T.T.H. and N.B. performed the ^{64}Cu radiolabeling studies. L.S., B.E.R., E.T., and L.M.M. wrote the manuscript and Supplementary Information, and all authors contributed to and approved the final version of the manuscript for submission.

ORCID

Liviu Mirica: 0000-0003-0584-9508

Emad Tajkhorshid: 0000-0001-8434-1010

Liang Sun: 0000-0002-0080-0855

Yiran Huang: 0000-0003-1755-9874

Andres Santiago Arango: 0000-0003-2278-3619

Soumyo Sen: 0000-0003-1607-9385

Notes

The authors declare no competing financial interest.

References

1. 2020 Alzheimer's disease facts and figures. *Alzheimer's & Dementia* **16**, 391-460.
2. Perrin, R. J.; Fagan, A. M.; Holtzman, D. M., Multimodal techniques for diagnosis and prognosis of Alzheimer's disease. *Nature* **2009**, *461* (7266), 916-922.
3. Selkoe, D. J., Resolving controversies on the path to Alzheimer's therapeutics. *Nat. Med.* **2011**, *17* (9), 1060-1065.
4. Karran, E.; Mercken, M.; Strooper, B. D., The Amyloid Cascade Hypothesis for Alzheimer's Disease: An Appraisal for the Development of Therapeutics. *Nat. Rev. Drug Discovery* **2011**, *10* (9), 698-712.
5. Chow, V. W.; Mattson, M. P.; Wong, P. C.; Gleichmann, M., An Overview of APP Processing Enzymes and Products. *NeuroMol. Med.* **2010**, *12* (1), 1-12.
6. Hardy, J. A.; Higgins, G. A., Alzheimer's Disease: The Amyloid Cascade Hypothesis. *Science* **1992**, *256* (5054), 184-185.
7. Bush, A. I., Metals and neuroscience. *Curr. Opin. Chem. Biol.* **2000**, *4* (2), 184-191.
8. Cleary, J. P.; Walsh, D. M.; Hofmeister, J. J.; Shankar, G. M.; Kuskowski, M. A.; Selkoe, D. J.; Ashe, K. H., Natural oligomers of the amyloid-beta protein specifically disrupt cognitive function. *Nat. Neurosci.* **2005**, *8* (1), 79-84.
9. Benilova, I.; Karran, E.; De Strooper, B., The Toxic A β Oligomer and Alzheimer's Disease: An Emperor in Need of Clothes. *Nat. Neurosci.* **2012**, *15*, 349-357.
10. Aliyan, A.; Cook, N. P.; Marti, A. A., Interrogating Amyloid Aggregates using Fluorescent Probes. *Chem. Rev.* **2019**, *119* (23), 11819-11856.
11. Xu, M. M.; Ren, W. M.; Tang, X. C.; Hu, Y. H.; Zhang, H. Y., Advances in development of fluorescent probes for detecting amyloid-beta aggregates. *Acta Pharmacol. Sin.* **2016**, *37* (6), 719-30.
12. Yang, J.; Zeng, F. T.; Ge, Y. R.; Peng, K. W.; Li, X. F.; Li, Y. Y.; Xu, Y. G., Development of Near-Infrared Fluorescent Probes for Use in Alzheimers Disease Diagnosis. *Bioconjugate Chem.* **2020**, *31* (1), 2-15.
13. Cao, K.; Farahi, M.; Dakanali, M.; Chang, W. M.; Sigurdson, C. J.; Theodorakis, E. A.; Yang, J., Aminonaphthalene 2-Cyanoacrylate (ANCA) Probes Fluorescently Discriminate between Amyloid-beta and Prion Plaques in Brain. *J. Am. Chem. Soc.* **2012**, *134* (42), 17338-17341.
14. Klunk, W. E.; Engler, H.; Nordberg, A.; Wang, Y.; Blomqvist, G.; Holt, D. P.; Bergström, M.; Savitcheva, I.; Huang, G.-F.; Estrada, S.; Ausén, B.; Debnath, M. L.; Barletta, J.; Price, J. C.; Sandell, J.; Lopresti, B. J.; Wall, A.; Koivisto, P.; Antoni, G.; Mathis, C. A.; Långström, B., Imaging Brain Amyloid in Alzheimer's Disease with Pittsburgh Compound-B. *Ann. Neurol.* **2004**, *55* (3), 306-319.
15. Kung, H. F.; Choi, S. R.; Qu, W.; Zhang, W.; Skovronsky, D., ¹⁸F Stilbenes and Styrylpyridines for PET Imaging of A β Plaques in Alzheimer's Disease: A Miniperspective. *J. Med. Chem.* **2010**, *53* (3), 933-941.
16. Herholz, K.; Ebmeier, K., Clinical amyloid imaging in Alzheimer's disease. *Lancet Neurol.* **2011**, *10* (7), 667-70.

17. Teoh, C. L.; Su, D.; Sahu, S.; Yun, S. W.; Drummond, E.; Prelli, F.; Lim, S.; Cho, S.; Ham, S.; Wisniewski, T.; Chang, Y. T., Chemical Fluorescent Probe for Detection of Abeta Oligomers. *J. Am. Chem. Soc.* **2015**, *137* (42), 13503-9.
18. Li, Y.; Xu, D.; Sun, A.; Ho, S. L.; Poon, C. Y.; Chan, H. N.; Ng, O. T. W.; Yung, K. K. L.; Yan, H.; Li, H. W.; Wong, M. S., Fluoro-substituted cyanine for reliable in vivo labelling of amyloid-beta oligomers and neuroprotection against amyloid-beta induced toxicity. *Chem. Sci.* **2017**, *8* (12), 8279-8284.
19. Lv, G.; Sun, A.; Wei, P.; Zhang, N.; Lan, H.; Yi, T., A spiropyran-based fluorescent probe for the specific detection of beta-amyloid peptide oligomers in Alzheimer's disease. *Chem. Comm.* **2016**, *52* (57), 8865-8868.
20. Li, Y.; Yang, J.; Liu, H.; Yang, J.; Du, L.; Feng, H.; Tian, Y.; Cao, J.; Ran, C., Tuning the stereo-hindrance of a curcumin scaffold for the selective imaging of the soluble forms of amyloid beta species. *Chem. Sci.* **2017**, *8* (11), 7710-7717.
21. Yang, J.; Zeng, F.; Li, X.; Ran, C.; Xu, Y.; Li, Y., Highly Specific Detection of A β Oligomers in Early Alzheimer's Disease by a Near-Infrared Fluorescent Probe with a "V-shaped" Spatial Conformation. *Chem. Comm.* **2020**, *56* (4), 583-586.
22. Liu, H. W.; Yang, J.; Wang, L. T.; Xu, Y. G.; Zhang, S. Y.; Lv, J.; Ran, C. Z.; Li, Y. Y., Targeting beta-amyloid plaques and oligomers: development of near-IR fluorescence imaging probes. *Future Med. Chem.* **2017**, *9* (2), 179-198.
23. Lee, S. J. C.; Nam, E.; Lee, H. J.; Savelieff, M. G.; Lim, M. H., Towards an understanding of amyloid-beta oligomers: characterization, toxicity mechanisms, and inhibitors. *Chem. Soc. Rev.* **2017**, *46* (2), 310-323.
24. Lv, G. L.; Sun, A. Y.; Wang, M. Q.; Wei, P.; Li, R. H.; Yi, T., A novel near-infrared fluorescent probe for detection of early-stage A β protofibrils in Alzheimer's disease. *Chem. Comm.* **2020**, *56* (11), 1625-1628.
25. Han, J.; Lee, H. J.; Kim, K. Y.; Nam, G.; Chae, J.; Lim, M. H., Mechanistic approaches for chemically modifying the coordination sphere of copper-amyloid-beta complexes. *Proc. Natl. Acad. Sci. U. S. A.* **2020**, *117* (10), 5160-5167.
26. Sharma, A. K.; Schultz, J. W.; Prior, J. T.; Rath, N. P.; Mirica, L. M., Coordination Chemistry of Bifunctional Chemical Agents Designed for Applications in (64)Cu PET Imaging for Alzheimer's Disease. *Inorg. Chem.* **2017**, *56* (22), 13801-13814.
27. Sharma, A. K.; Kim, J.; Prior, J. T.; Hawco, N. J.; Rath, N. P.; Kim, J.; Mirica, L. M., Small Bifunctional Chelators That Do Not Disaggregate Amyloid β Fibrils Exhibit Reduced Cellular Toxicity. *Inorg. Chem.* **2014**, *53* (21), 11367-11376.
28. Sharma, A. K.; Pavlova, S. T.; Kim, J.; Finkelstein, D.; Hawco, N. J.; Rath, N. P.; Kim, J.; Mirica, L. M., Bifunctional Compounds for Controlling Metal-mediated Aggregation of the A β ₄₂ Peptide. *J. Am. Chem. Soc.* **2012**, *134* (15), 6625-6636.
29. Beck, M. W.; Oh, S. B.; Kerr, R. A.; Lee, H. J.; Kim, S. H.; Kim, S.; Jang, M.; Ruotolo, B. T.; Lee, J.-Y.; Lim, M. H., A rationally designed small molecule for identifying an in vivo link between metal-amyloid-b complexes and the pathogenesis of Alzheimer's disease. *Chem. Sci.* **2015**, *6* (3), 1879-1886.
30. Beck, M. W.; Derrick, J. S.; Kerr, R. A.; Oh, S. B.; Cho, W. J.; Lee, S. J. C.; Ji, Y.; Han, J.; Tehrani, Z. A.; Suh, N.; Kim, S.; Larsen, S. D.; Kim, K. S.; Lee, J. Y.; Ruotolo, B. T.; Lim, M. H., Structure-mechanism-based engineering of chemical regulators targeting distinct pathological factors in Alzheimer's disease. *Nat. Commun.* **2016**, *7*, 13115.
31. Yang, J.; Zhang, X. L.; Yuan, P.; Yang, J.; Xu, Y. G.; Grutzendler, J.; Shao, Y. H.; Moore, A.; Ran, C. Z., Oxalate-curcumin-based probe for micro- and macroimaging of reactive oxygen species in Alzheimer's disease. *Proc. Natl. Acad. Sci. U. S. A.* **2017**, *114* (47), 12384-12389.
32. Yang, J.; Yang, J.; Liang, S. H.; Xu, Y. G.; Moore, A.; Ran, C. Z., Imaging hydrogen peroxide in Alzheimer's disease via cascade signal amplification. *Sci. Rep.* **2016**, *6*, 35613.

33. Gomes, L. M. F.; Mahammed, A.; Prosser, K. E.; Smith, J. R.; Silverman, M. A.; Walsby, C. J.; Gross, Z.; Storr, T., A catalytic antioxidant for limiting amyloid-beta peptide aggregation and reactive oxygen species generation. *Chem. Sci.* **2019**, *10* (6), 1634-1643.
34. Li, L.; Xu, S.; Liu, L.; Feng, R.; Gong, Y.; Zhao, X.; Li, J.; Cai, J.; Feng, N.; Wang, L.; Wang, X.; Peng, Y., Multifunctional Compound AD-35 Improves Cognitive Impairment and Attenuates the Production of TNF-alpha and IL-1beta in an Abeta25-35-induced Rat Model of Alzheimer's Disease. *J Alzheimers Dis* **2017**, *56* (4), 1403-1417.
35. Moussa, C.; Hebron, M.; Huang, X.; Ahn, J.; Rissman, R. A.; Aisen, P. S.; Turner, R. S., Resveratrol regulates neuro-inflammation and induces adaptive immunity in Alzheimer's disease. *J Neuroinflamm* **2017**, *14*:1.
36. Camps, P.; Formosa, X.; Galdeano, C.; Gomez, T.; Munoz-Torrero, D.; Scarpellini, M.; Viayna, E.; Badia, A.; Clos, M. V.; Camins, A.; Pallas, M.; Bartolini, M.; Mancini, F.; Andrisano, V.; Estelrich, J.; Lizondo, M.; Bidon-Chanal, A.; Luque, F. J., Novel donepezil-based inhibitors of acetyl- and butyrylcholinesterase and acetylcholinesterase-induced beta-amyloid aggregation. *J. Med. Chem.* **2008**, *51* (12), 3588-3598.
37. Piazza, L.; Rampa, A.; Bisi, A.; Gobbi, S.; Belluti, F.; Cavalli, A.; Bartolini, M.; Andrisano, V.; Valenti, P.; Recanatini, M., 3-(4-{{benzyl(methyl)amino}methyl}-phenyl)-6,7-dimethoxy-2H-2-chromenone (AP2238) inhibits both acetylcholinesterase and acetylcholinesterase-induced beta-amyloid aggregation: A dual function lead for Alzheimer's disease therapy. *J. Med. Chem.* **2003**, *46* (12), 2279-2282.
38. Savelieff, M. G.; Nam, G.; Kang, J.; Lee, H. J.; Lee, M.; Lim, M. H., Development of Multifunctional Molecules as Potential Therapeutic Candidates for Alzheimer's Disease, Parkinson's Disease, and Amyotrophic Lateral Sclerosis in the Last Decade. *Chem. Rev.* **2019**, *119* (2), 1221-1322.
39. Jones, M. R.; Mathieu, E.; Dyrager, C.; Faissner, S.; Vaillancourt, Z.; Korshavn, K. J.; Lim, M. H.; Ramamoorthy, A.; Wee Yong, V.; Tsutsui, S.; Stys, P. K.; Storr, T., Multi-target-directed phenol-triazole ligands as therapeutic agents for Alzheimer's disease. *Chem. Sci.* **2017**, *8* (8), 5636-5643.
40. Kim, M.; Kang, J.; Lee, M.; Han, J.; Nam, G.; Tak, E.; Kim, M. S.; Lee, H. J.; Nam, E.; Park, J.; Oh, S. J.; Lee, J. Y.; Lee, J. Y.; Baik, M. H.; Lim, M. H., Minimalistic Principles for Designing Small Molecules with Multiple Reactivities against Pathological Factors in Dementia. *J. Am. Chem. Soc.* **2020**, *142* (18), 8183-8193.
41. Huang, Y. R.; Cho, H. J.; Bandara, N.; Sun, L.; Tran, D.; Rogers, B. E.; Mirica, L. M., Metal-chelating benzothiazole multifunctional compounds for the modulation and Cu-64 PET imaging of A beta aggregation. *Chem. Sci.* **2020**, *11* (30), 7789-7799.
42. Cho, H.-J.; Sharma, A. K.; Zhang, Y.; Gross, M. L.; Mirica, L. M., A Multifunctional Chemical Agent as an Attenuator of Amyloid Burden and Neuroinflammation in Alzheimer's Disease. *ACS Chem. Neurosci.* **2020**, *11* (10), 1471-1481.
43. Serra-Batiste, M.; Ninot-Pedrosa, M.; Bayoumi, M.; Gairi, M.; Maglia, G.; Carulla, N., A beta 42 assembles into specific beta-barrel pore-forming oligomers in membrane-mimicking environments. *Proc. Natl. Acad. Sci. U. S. A.* **2016**, *113* (39), 10866-10871.
44. Ciudad, S.; Puig, E.; Botzanowski, T.; Meigooni, M.; Arango, A. S.; Do, J.; Mayzel, M.; Bayoumi, M.; Chaignepain, S.; Maglia, G.; Cianferani, S.; Orekhov, V.; Tajkhorshid, E.; Bardiaux, B.; Carulla, N., Abeta(1-42) tetramer and octamer structures reveal edge conductivity pores as a mechanism for membrane damage. *Nat. Commun.* **2020**, *11* (1), 3014.
45. Ahmed, M.; Davis, J.; Aucoin, D.; Sato, T.; Ahuja, S.; Aimoto, S.; Elliott, J. I.; Van Nostrand, W. E.; Smith, S. O., Structural conversion of neurotoxic amyloid-beta(1-42) oligomers to fibrils. *Nat. Struct. Mol. Biol.* **2010**, *17* (5), 561-7.
46. Arispe, N.; Rojas, E.; Pollard, H. B., Alzheimer-Disease Amyloid Beta-Protein Forms Calcium Channels in Bilayer-Membranes - Blockade by Tromethamine and Aluminum. *Proc. Natl. Acad. Sci. U. S. A.* **1993**, *90* (2), 567-571.
47. Arispe, N.; Pollard, H. B.; Rojas, E., Zn²⁺ interaction with Alzheimer amyloid beta protein calcium channels. *Proc. Natl. Acad. Sci. U. S. A.* **1996**, *93* (4), 1710-1715.

48. Hirakura, Y.; Lin, M. C.; Kagan, B. L., Alzheimer amyloid A beta 1-42 channels: Effects of solvent, pH, and congo red. *J. Neurosci. Res.* **1999**, *57* (4), 458-466.
49. Lin, H.; Bhatia, R.; Lal, R., Amyloid beta protein forms ion channels: implications for Alzheimer's disease pathophysiology. *FASEB J.* **2001**, *15* (13), 2433-2444.
50. Kourie, J. I.; Henry, C. L.; Farrelly, P., Diversity of amyloid beta protein fragment [1-40]-formed channels. *Cell Mol Neurobiol* **2001**, *21* (3), 255-284.
51. Le Fur, M.; Beyler, M.; Le Poul, N.; Lima, L. M. P.; Le Mest, Y.; Delgado, R.; Platas-Iglesias, C.; Patinec, V.; Tripier, R., Improving the stability and inertness of Cu(II) and Cu(I) complexes with methylthiazolyl ligands by tuning the macrocyclic structure. *Dalton Trans.* **2016**, *45* (17), 7406-7420.
52. Gotzmann, C.; Braun, F.; Bartholoma, M. D., Synthesis, Cu-64-labeling and PET imaging of 1,4,7-triazacyclononane derived chelators with pendant azaheterocyclic arms. *RSC Adv.* **2016**, *6* (1), 119-131.
53. Flaherty, D. P.; Kiyota, T.; Dong, Y. X.; Ikezu, T.; Vennerstrom, J. L., Phenolic Bis-styrylbenzenes as beta-Amyloid Binding Ligands and Free Radical Scavengers. *J. Med. Chem.* **2010**, *53* (22), 7992-7999.
54. Boländer, A.; Kieser, D.; Scholz, C.; Heyny-von Haußen, R.; Mall, G.; Goetschy, V.; Czech, C.; Schmidt, B., Synthesis of Methoxy-X04 Derivatives and Their Evaluation in Alzheimer's Disease Pathology. *Neurodegenerative Diseases* **2014**, *13* (4), 209-213.
55. Necula, M.; Kayed, R.; Milton, S.; Glabe, C. G., Small molecule inhibitors of aggregation indicate that amyloid β oligomerization and fibrillization pathways are independent and distinct. *J. Biol. Chem.* **2007**, *282* (14), 10311-10324.
56. Miller, E. W.; Lin, J. Y.; Frady, E. P.; Steinbach, P. A.; Kristan, W. B.; Tsien, R. Y., Optically monitoring voltage in neurons by photo-induced electron transfer through molecular wires. *Proc. Natl. Acad. Sci. U. S. A.* **2012**, *109* (6), 2114-2119.
57. Li, H. J.; Wang, L., Triethanolamine as an efficient and reusable base, ligand and reaction medium for phosphane-free palladium-catalyzed Heck reactions. *Eur. J. Org. Chem.* **2006**, (22), 5099-5102.
58. Klein, W. L.; Krafft, G. A.; Finch, C. E., Targeting small A beta oligomers: the solution to an Alzheimer's disease conundrum? *Trends Neurosci.* **2001**, *24* (4), 219-224.
59. Oakley, H.; Cole, S. L.; Logan, S.; Maus, E.; Shao, P.; Craft, J.; Guillozet-Bongaarts, A.; Ohno, M.; Disterhoft, J.; Van Eldik, L.; Berry, R.; Vassar, R., Intraneuronal β -amyloid aggregates, neurodegeneration, and neuron loss in transgenic mice with five familial Alzheimer's disease mutations: potential factors in amyloid plaque formation. *J. Neurosci.* **2006**, *26* (40), 10129-10140.
60. Wilcock, D. M.; Gordon, M. N.; Morgan, D., Quantification of cerebral amyloid angiopathy and parenchymal amyloid plaques with Congo red histochemical stain. *Nat. Protoc.* **2006**, *1* (3), 1591-1595.
61. Schwetye, K. E.; Cirrito, J. R.; Esparza, T. J.; Mac Donald, C. L.; Holtzman, D. M.; Brody, D. L., Traumatic Brain Injury Reduces Soluble Extracellular Amyloid- β in Mice: A Methodologically Novel Combined Microdialysis-Controlled Cortical Impact Study. *Neurobiol. Dis.* **2010**, *40* (3), 555-564.
62. Lindhagen-Persson, M.; Brannstrom, K.; Vestling, M.; Steinitz, M.; Olofsson, A., Amyloid-beta oligomer specificity mediated by the IgM isotype--implications for a specific protective mechanism exerted by endogenous auto-antibodies. *PLoS One* **2010**, *5* (11), e13928.
63. Re, R.; Pellegrini, N.; Proteggente, A.; Pannala, A.; Yang, M.; Rice-Evans, C., Antioxidant activity applying an improved ABTS radical cation decolorization assay. *Free Radic. Biol. Med.* **1999**, *26* (9), 1231-1237.
64. Huang, D. J.; Ou, B. X.; Prior, R. L., The chemistry behind antioxidant capacity assays. *J. Agric. Food Chem.* **2005**, *53* (6), 1841-1856.
65. Saharan, S.; Mandal, P. K., The emerging role of glutathione in Alzheimer's disease. *J Alzheimers Dis* **2014**, *40* (3), 519-29.
66. Conte-Daban, A.; Beyler, M.; Tripier, R.; Hureau, C., Kinetics Are Crucial When Targeting Copper Ions to Fight Alzheimer's Disease: An Illustration with Azamacrocyclic Ligands. *Chem. Eur. J.* **2018**, *24* (33), 8447-8452.

67. Sharma, A. K.; Pavlova, S. T.; Kim, J.; Kim, J.; Mirica, L. M., The effect of Cu²⁺ and Zn²⁺ on the Aβ₄₂ peptide aggregation and cellular toxicity. *Metallomics* **2013**, 5 (11), 1529-1536.
68. Dahlgren, K. N.; Manelli, A. M.; Stine, W. B.; Baker, L. K.; Krafft, G. A.; LaDu, M. J., Oligomeric and fibrillar species of amyloid-beta peptides differentially affect neuronal viability. *J. Biol. Chem.* **2002**, 277 (35), 32046-32053.
69. Dischino, D. D.; Welch, M. J.; Kilbourn, M. R.; Raichle, M. E., Relationship between Lipophilicity and Brain Extraction of C-11-Labeled Radiopharmaceuticals. *J. Nucl. Med.* **1983**, 24 (11), 1030-1038.
70. Ohno, M.; Chang, L.; Tseng, W.; Oakley, H.; Citron, M.; Klein, W. L.; Vassar, R.; Disterhoft, J. F., Temporal memory deficits in Alzheimer's mouse models: rescue by genetic deletion of BACE1. *Eur. J. Neurosci.* **2006**, 23 (1), 251-260.
71. Makin, S., The amyloid hypothesis on trial. *Nature* **2018**, 559 (7715), S4-S4.
72. Morris, G. P.; Clark, I. A.; Vissel, B., Inconsistencies and Controversies Surrounding the Amyloid Hypothesis of Alzheimer's Disease. *Acta. Neuropathol. Commun.* **2014**, 2 (1), 135.
73. He, Z.; Guo, J. L.; McBride, J. D.; Narasimhan, S.; Kim, H.; Changolkar, L.; Zhang, B.; Gathagan, R. J.; Yue, C.; Dengler, C.; Stieber, A.; Nitla, M.; Coulter, D. A.; Abel, T.; Brunden, K. R.; Trojanowski, J. Q.; Lee, V. M. Y., Amyloid-β plaques enhance Alzheimer's brain tau-seeded pathologies by facilitating neuritic plaque tau aggregation. *Nat. Med.* **2017**, 24, 29.
74. Leyns, C. E. G.; Gratuze, M.; Narasimhan, S.; Jain, N.; Koscal, L. J.; Jiang, H.; Manis, M.; Colonna, M.; Lee, V. M. Y.; Ulrich, J. D.; Holtzman, D. M., TREM2 function impedes tau seeding in neuritic plaques. *Nat. Neurosci.* **2019**, 22 (8), 1217-1222.
75. Shukla, V.; Zheng, Y.-L.; Mishra, S. K.; Amin, N. D.; Steiner, J.; Grant, P.; Kesavapany, S.; Pant, H. C., A truncated peptide from p35, a Cdk5 activator, prevents Alzheimer's disease phenotypes in model mice. *The FASEB Journal* **2013**, 27 (1), 174-186.
76. Giacobini, E.; Gold, G., Alzheimer disease therapy—moving from amyloid-β to tau. *Nat. Rev. Neurol.* **2013**, 9 (12), 677-686.
77. Ostrowitzki, S.; Deptula, D.; Thurfjell, L.; Barkhof, F.; Bohrmann, B.; Brooks, D. J.; Klunk, W. E.; Ashford, E.; Yoo, K.; Xu, Z.-X.; Loetscher, H.; Santarelli, L., Mechanism of amyloid removal in patients with Alzheimer disease treated with Gantenerumab. *JAMA Neurol.* **2012**, 69 (2), 198-207.
78. Doody, R. S.; Thomas, R. G.; Farlow, M.; Iwatsubo, T.; Vellas, B.; Joffe, S.; Kieburtz, K.; Raman, R.; Sun, X.; Aisen, P. S.; Siemers, E.; Liu-Seifert, H.; Mohs, R., Phase 3 trials of Solanezumab for mild-to-moderate Alzheimer's disease. *N. Engl. J. Med.* **2014**, 370 (4), 311-321.
79. Salloway, S.; Sperling, R.; Fox, N. C.; Blennow, K.; Klunk, W.; Raskind, M.; Sabbagh, M.; Honig, L. S.; Porsteinsson, A. P.; Ferris, S.; Reichert, M.; Ketter, N.; Nejadnik, B.; Guenzler, V.; Miloslavsky, M.; Wang, D.; Lu, Y.; Lull, J.; Tudor, I. C.; Liu, E.; Grundman, M.; Yuen, E.; Black, R.; Brashear, H. R., Two phase 3 trials of Bapineuzumab in mild-to-moderate Alzheimer's disease. *N. Engl. J. Med.* **2014**, 370 (4), 322-333.
80. Dhawan, G.; Floden, A. M.; Combs, C. K., Amyloid-beta oligomers stimulate microglia through a tyrosine kinase dependent mechanism. *Neurobiol. Aging* **2012**, 33 (10), 2247-2261.
81. Doens, D.; Fernandez, P. L., Microglia receptors and their implications in the response to amyloid beta for Alzheimer's disease pathogenesis. *J Neuroinflamm* **2014**, 11:48.
82. Phillips, J. C.; Braun, R.; Wang, W.; Gumbart, J.; Tajkhorshid, E.; Villa, E.; Chipot, C.; Skeel, R. D.; Kale, L.; Schulten, K., Scalable molecular dynamics with NAMD. *J. Comput. Chem.* **2005**, 26 (16), 1781-802.
83. Phillips, J. C.; Hardy, D. J.; Maia, J. D. C.; Stone, J. E.; Ribeiro, J. V.; Bernardi, R. C.; Buch, R.; Fiorin, G.; Henin, J.; Jiang, W.; McGreevy, R.; Melo, M. C. R.; Radak, B. K.; Skeel, R. D.; Singharoy, A.; Wang, Y.; Roux, B.; Aksimentiev, A.; Luthey-Schulten, Z.; Kale, L. V.; Schulten, K.; Chipot, C.; Tajkhorshid, E., Scalable molecular dynamics on CPU and GPU architectures with NAMD. *J. Chem. Phys.* **2020**, 153 (4).
84. Paravastu, A. K.; Leapman, R. D.; Yau, W. M.; Tycko, R., Molecular structural basis for polymorphism in Alzheimer's beta-amyloid fibrils. *Proc. Natl. Acad. Sci. U. S. A.* **2008**, 105 (47), 18349-18354.

85. Hickey, J. L.; Lim, S.; Hayne, D. J.; Paterson, B. M.; White, J. M.; Villemagne, V. L.; Roselt, P.; Binns, D.; Cullinane, C.; Jeffery, C. M.; Price, R. I.; Barnham, K. J.; Donnelly, P. S., Diagnostic Imaging Agents for Alzheimer's Disease: Copper Radiopharmaceuticals that Target A β Plaques. *J. Am. Chem. Soc.* **2013**, *135* (43), 16120-16132.
86. McInnes, L. E.; Noor, A.; Kysenius, K.; Cullinane, C.; Roselt, P.; McLean, C. A.; Chiu, F. C. K.; Powell, A. K.; Crouch, P. J.; White, J. M.; Donnelly, P. S., Potential Diagnostic Imaging of Alzheimer's Disease with Copper-64 Complexes That Bind to Amyloid-beta Plaques. *Inorg. Chem.* **2019**, *58* (5), 3382-3395.
87. Bandara, N.; Sharma, A. K.; Krieger, S.; Schultz, J. W.; Han, B. H.; Rogers, B. E.; Mirica, L. M., Evaluation of ⁶⁴Cu-based Radiopharmaceuticals That Target A β Peptide Aggregates as Diagnostic Tools for Alzheimer's Disease. *J. Am. Chem. Soc.* **2017**, *139* (36), 12550-12558.
88. Noor, A.; Hayne, D. J.; Lim, S.; Van Zuylekom, J. K.; Cullinane, C.; Roselt, P. D.; McLean, C. A.; White, J. M.; Donnelly, P. S., Copper Bis(thiosemicarbazonato)-stilbenyl Complexes That Bind to Amyloid-beta Plaques. *Inorg. Chem.* **2020**, *59* (16), 11658-11669.
89. Cho, H. J.; Huynh, T. T.; Rogers, B. E.; Mirica, L. M., Design of a multivalent bifunctional chelator for diagnostic (⁶⁴Cu) PET imaging in Alzheimer's disease. *Proc Natl Acad Sci U S A* **2020**, *117* (49), 30928-30933.

TOC Graphical abstract

